Rotor Blade Harmonic Air Loading

R. H. Miller*
Massachusetts Institute of Technology, Cambridge, Mass.

The determination of the air loads acting on rotor blades in forward flight presents an interesting and challenging problem in applied aerodynamics. Of particular importance for design purposes are the oscillatory components of this loading occurring at harmonics of the rotor speed. Unlike a wing, the trailing and shed vortex system of the blade generates a spiral wake that returns close to the blade. Because of its close proximity to the blade, the wake cannot be considered as rigid. Also, since the resulting loads are highly time-dependent, unsteady aerodynamic effects become important. An analytical treatment for the limiting case of hovering flight results in a simple closed-form solution that demonstrates that the oscillatory lift under normal operating conditions can be less than 50% of its quasi-static value. It is shown that the air loads in forward flight depend primarily on the equivalent lift deficiency and the downwash generated by the steady-state blade vortex system. It is also shown that, at low speeds, the rotor wake can be drawn up into the rotor leading edge and that this is probably the primary cause of transition roughness and noise encountered under certain flight conditions.

Nomenclature

A_n = coefficients of chordwise vorticity distribution
$A_{ncl}{}^k$ = coefficient of cosine component of kth harmonic of circulation or downwash at station l due to a $\cos n\phi$ variation of shed wake vortex strength
$B_{nsl}{}^k$ = same, except sine component due to a $\sin n\phi$ input
$P_{ncl}{}^k$ $Q_{nsl}{}^k$ = same, except due to trailing wake
$C(k,m,h)$, $C(k)$,C = lift deficiency function
C_n = kI_c
C_T = thrust coefficient $= T/\pi\rho\Omega^2R^4$
$F(\phi)$ = integrand for far shed wake
I_c, I_s = integrals defining blade circulation due to near shed wake
I_c', I_s' = integrals defining blade lift due to near shed wake
L = lift
LN = blade Lock number (inertia parameter)
Q = number of blades
R = rotor radius
S_n = kI_s
T = rotor thrust
V = forward velocity
a = distance between center of twist and center of airfoil, positive aft
a_n = blade flapping angle (cosine component)
b = blade semichord
b_n = blade flapping angle (sine component)
d = horizontal distance traveled by rotor hub
$f(\phi)$ = integrand for trailing wake
$g(\phi)$ = integrand for shed wake after integration over l
h = wake spacing
h^* = bh
i = angle between rotor disk and relative wind, positive nose up
k = $nb/\eta R = \omega b/\Omega R\eta$ = reduced frequency
l = rotor span parameter
m = number of wake spirals (also used for frequency ratio in two-dimensional solution)
n = harmonic of rotor speed (also used for wake identification in two-dimensional solution)
u = velocity at airfoil due to airfoil motion
v = induced velocity due to blade-distributed vorticity
w = induced velocity at blade due to wake
x = distance along blade chord, nondimensionalized with respect to R unless starred
z = vertical distance traveled by rotor hub
Γ = vorticity or circulation
Ω = rotational speed
α = angle of attack
α_T = blade tip angle of attack
β = blade flapping angle $= a_0 - \sum_{n=1}^{\infty} a_n \cos n\psi + b_n \sin n\psi$
γ = element of distributed vorticity
γ_n = nondimensional form of blade circulation $= \Gamma_n/2\pi b\Omega R$
γ_r = coefficient of series for blade spanwise circulation
ζ = blade spacing
η = rotor span parameter; also chordwise distance in Appendix
λ = inflow normal to rotor disk
χ = distance from reference point on blade to trailing edge
μ = advance ratio $= V\cos i/\Omega R$
ξ = distance to element of vorticity in wake
ξ^* = $b\xi$
ρ = density of air
σ = rotor solidity
ϕ = azimuth of wake measured from downwind position; also used for velocity potential in Appendix
ψ = rotor azimuth measured from blade downwind position

Subscripts

q = quasi-static
N = near
F = far
nc = cosine n input
ns = sine n input

Superscripts

S = shed
T = trailing

Presented as Preprint 62-82 at the IAS 30th Annual Meeting, New York, January 22–24, 1962; revision received April 20, 1964. This work was initially supported by funds from the Carnegie Research Fund, and computer time was made available by the Computation Center at Massachusetts Institute of Technology. The program is currently under sponsorship of the Department of the Navy, Bureau of Naval Weapons. The author wishes to express appreciation to Nancy Ghoreeb, who programed the computations.

* Slater Professor of Flight Transportation, Department of Aeronautics and Astronautics. Fellow Member AIAA.

Introduction

THE rapid increase in VTOL technology has brought with it the realization that many of the basic approximations inherent in classical aerodynamic wing theory, such as the concepts of a wake remaining in the plane of the airfoil, of induced velocities small compared to forward velocities, possibly even the concept of a "rigid" wake and the neglect of vortex-vortex interaction, must all be re-examined when the vertical velocity that generates lift is large compared to the forward flight velocity, as happens in the case of a lifting jet immersed in a wing or for a helicopter rotor in low-speed forward flight.

A particularly interesting example is the determination of the air loads acting on a rotor blade in forward flight. The oscillatory air loads occurring at harmonics of the rotor speed are the primary source of the blade stresses that establish the fatigue lift of the structure and of the periodic hub loads that determine the fuselage vibration level. The simple theory of rotor blade loading in forward flight in which a uniform or triangular inflow distribution is assumed indicates that these loadings will decrease as μ^n, where μ is the advance ratio and n indicates the nth harmonic of loading. This does not fit the observed facts, since harmonics as high as the fifth or sixth are known to produce appreciable blade stresses and vibratory shaft loads at advance ratios of the order of $\mu = 0.1$ or 0.2, where the simplified theory would indicate such loadings to be negligible (see, for example, Ref. 2). The higher harmonic components of the air loading must, therefore, arise primarily from a nonuniform downwash at the rotor disk generated by the rotor wake. Their analytical determination requires some means of computing this downwash which takes into account both the spiral wake geometry, its effects on the individual blades, and the unsteady aerodynamic effects associated with the blade passage through this variable velocity field, which Ref. 1 has shown to be of primary importance in the presence of a returning wake.

This, however, is only part of the problem since, once the aerodynamic excitation is established, the response of the blade to the excitation must be determined, and this, in turn, introduces a complicated aeroelastic problem in which the blade flexibility must be considered as well as the effects of the powerful pitch flap coupling that occurs when the rotor blade bends out of the plane of the feathering axis. It is shown in Ref. 3 that this type of coupling is of considerable importance and could, in turn, appreciably modify the excitation. Consequently, an exact solution requires that the problem be solved as a whole rather than separately for the aerodynamic input and then for the dynamic response. However, certainly the first step is the definition of the air loading, since this is the primary forcing function.

The time-averaged velocities induced by the rotor wake in forward flight have been computed in Refs. 4–9 using the assumption of an infinite number of blades and a prescribed loading on the disk. In Ref. 10 the semi-infinite vortex cylinder was replaced by segments of infinite straight trailing wakes oriented below the rotor, and the techniques developed in the quasi-static lifting-line theory for fixed wings were used to compute the loading. The local downwash induced by a finite trailing wake of spiral form and constant strength was analyzed in Ref. 11, where it was shown that a highly time-dependent interference velocity is generated as the blade passes over the returning wake.

In Ref. 1, it was shown that the lift deficiency function of classical two-dimensional nonstationary flow theory, which accounts for the reduction in lift and phase shifts due to the shed wake, could approach very small values at integers of rotor speed when the effects of the returning shed wake were taken into consideration. Similar analyses are contained in Refs. 12 and 13. All of these analyses are limited to two-dimensional models and hovering flight. An extension to the three-dimensional case of a hovering rotor is contained in Ref. 14. The results of this analysis confirm experience with similar high-aspect-ratio fixed-wing solutions in which the two-dimensional model is found to be generally adequate for the prediction of the lift deficiency functions. A valuable contribution of Ref. 14 lies in its development of the concept of the rotor as operating in a straight "sheared" flow representing velocity variations along the blade span, a concept that is particularly useful in the development of the theory of this paper.

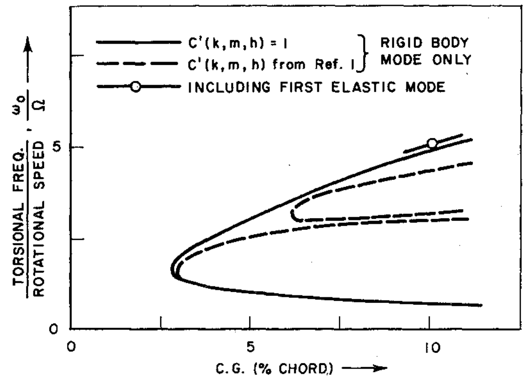

Fig. 1 Flutter boundaries in hovering showing comparison between unsteady aerodynamic and quasi-static theory.

In Ref. 3 the theory of Ref. 1 was applied to the calculation of blade stability. Figure 1, taken from Ref. 15, shows that neglect of the effects of the returning wake in such calculations is conservative since the exciting forces, as well as the damping forces, are reduced by wake interference effects. Experimental verification of these effects was obtained in the tests reported in Ref. 16. When an attempt was made to excite the blade aerodynamically by harmonic pitch variation, no appreciable effects of the returning wake were noticed; however, with mechanical excitation of the rotor hub, a pronounced reduction in damping was evidenced by the large increase in blade response at harmonics of the rotor speed. This is shown in Fig. 2.

It is therefore clear that any attempt to predict the blade harmonic loading must treat the unsteady aerodynamic effects with some care. Furthermore, since a simple uniform wake theory cannot predict the observed order of magnitude of these loads, the mechanism of their generation must come from the harmonic content of the interference velocities generated at the rotor disk by the rotor wake. A three-dimensional model using finite number of blades is required if the harmonic content of this downwash is to be predicted with any degree of accuracy.

It is the purpose of this paper to present a solution to the problem of determining rotor blade harmonic loading which includes both the unsteady aerodynamic effects and the actual three-dimensional wake geometry. The problem is first formulated for the complete case of the three-dimensional rotor with a finite number of blades in forward flight. A method of solutions is then proposed which involves considering the spiral wake in two sections, the "near wake" in the immediate vicinity of the blade and the "far wake" con-

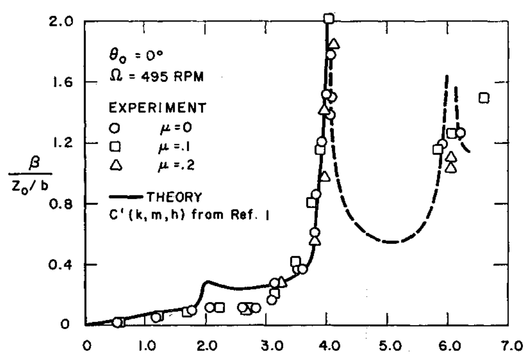

Fig. 2 Flapping response to sinusoidal vertical hub displacement as a function of frequency ratio for different advance ratios.

taining all of the remaining wake. The air loads on the blade generated by the near wake are treated using lifting-surface theories, whereas the far wake is treated using the lifting-line approximation. This suggested treatment is then evaluated by comparing the exact solutions given for the two-dimensional model in Ref. 1 with a similar solution using lifting-line theory for the equivalent far wake.

Analytical solutions are then obtained for the three-dimensional rotor in vertical flight. This results in a simple solution for the lift deficiency function and provides a useful check on the numerical solutions obtained using the complete theory.

Finally, the relationships required for the solution of the complete problem of the air loads on a three-dimensional rotor in forward flight are developed and used to examine various conditions representative of low-speed transition and cruise flight.

Formulation of Problem

For ease in representing the rotor blade and wake geometry, the blade will be assumed to consist of a sheet of distributed vorticity and the boundary conditions satisfied for the various vortex pairs consisting of the elements of wake vorticity and corresponding blade circulation. The distribution of strength along the trailing and shed vortex lines in the wake will be determined by the time variations in strength of the bound vortex from which they spring. The final lift and circulation on the blade section are obtained by summing the effects of all elements of vorticity.

The background development of the unsteady aerodynamic theory for wings is well covered in the literature, for example, Refs. 17–20. A brief derivation using the approach developed in this paper for the rotor is presented for the classical two-dimensional airfoil case in the Appendix, since it has been found convenient to modify slightly the familiar treatments when considering the three-dimensional rotor.

If the chordwise vorticity is represented by the series

$$\gamma(x) = A_0 \tan\frac{\theta}{2} + \sum_{n=1}^{\infty} A_n \sin n\theta$$

where $b \cos\theta = xR$ and b = half-chord, then the flow normal to the blade at a chordwise station x due to the total chordwise vorticity is

$$v(x) = \frac{A_0}{2} + \sum_{n=1}^{\infty} \frac{A_n}{2} \cos n\theta \quad (1)$$

and it is desired to satisfy the boundary conditions on the airfoil surface given by

$$v(x) + u(x) + w(x) = 0 \quad (2)$$

where $w(x)$ is the velocity at the airfoil induced by the wake, and $u(x)$ represents the velocity normal to the airfoil due to the angle of incidence and blade motion.

The blade is assumed to be rigid chordwise. Following the law of constancy of circulation, any change in circulation on the airfoil $d\Gamma_b$ must leave a counter vortex $\gamma d\xi$ shed in the wake such that

$$\gamma d\xi = -d\Gamma_b \quad (3)$$

The three-dimensional circulatory system of the wake and airfoil is completed by trailing vortex lines generated by changes in circulation along the blade span (see Fig. 3) and the corresponding bound vortex on the blade. Certain statements must now be made as to the nature of the wake vorticity.

First the concept of a "semirigid" wake will be introduced, i.e., every element of vorticity will be assumed to retain the instantaneous vertical velocity imparted to it at the moment it was shed or trailed. This establishes a spiral wake descending at every spanwise station with a constant velocity in time but permits different vertical velocities azimuthwise. The spiral sheet representing the wake thus continuously changes shape as it descends. Other than in establishing the instantaneous wake location, the effects of this wake velocity will be neglected (see Appendix). The effect of the wake on its own velocity will also be neglected. Changes in the mean velocity that establishes the spiral spacing as the wake descends are thus ignored as well as the tendency for vortex-vortex interaction of the individual spirals. Since the induced velocity at the rotor plane is determined primarily by the first few spirals, this assumption is believed to be valid. Furthermore, it is most probable that the vortex sheets will roll up and form two individual vortex lines in the fully developed wake as in the case of fixed-wing aircraft, particularly since a variable downward velocity decreasing toward the center of the rotor implies an eventual crossing and almost certain intermingling of the vortex sheets in the wake. Further refinement of the mathematical model does not, therefore, appear to be warranted at the present time.

Secondly, the assumption, inherent in all fixed-wing analyses, of a vortex strength constant in time will be made, that is, viscous effects will be ignored. Although this assumption is less satisfying for the case of the returning spiral wake of the relatively lightly loaded rotor than in the case of a wing in which the wake extends rearward to infinity or for a highly loaded propeller, it is consistent with the previous assumption and justifiable on the same basis.

Finally, the effect of wake-induced velocities in the plane of the blade will be ignored.

The basic relationship required to compute the downwash at the rotor disk for a three-dimensional rotor operating at an advance rotor μ will now be developed. The downwash generated by an element $\bar{ds}$ of a trailing vortex line with strength Γ at a distance $\bar{A}$ from the element is, in vector notation,

$$d\bar{q} = (\Gamma d\bar{s} \times \bar{A})/4\pi a^3$$

It will be assumed that the element of vorticity has been generated from the trailing edge of the blade at a spanwise station l from the center of rotation when the blade was at azimuth angle ϕ. The vertical component of downwash dw_1 which this element induces at another spanwise station η and chordwise station x of the blade when the blade has rotated to an azimuth angle ψ is

$$dw_1 = \frac{\Gamma}{4\pi R} \times \frac{ds_2 A_1 - ds_1 A_2}{(A_1^2 + A_2^2 + A_r^2)^{3/2}} = f(\phi)d\phi \quad (4)$$

where

$$ds_1 = \mu d\phi \cos\phi \qquad ds_2 = \mu d\phi \sin\phi + l d\phi$$

and

$$A_1 = l + d\cos\phi - \eta\cos(\psi - \phi) - x\sin(\psi - \phi)$$
$$A_2 = \chi + d\sin\phi + \eta\sin(\psi - \phi) - x\cos(\psi - \phi)$$
$$A_3 = -z$$

All distances are nondimensional in terms of blade radius R. x is a chordwise distance measured from a reference point on the blade, for example, the quarter-chord point, and χ is the distance from this point to the origin of the trailing vortex line. d is the distance traveled by the rotor hub during the time $t = (\psi - \phi)/\Omega$, and z is the vertical distance of the element of vorticity below the blade. If m is the number of wake spirals to be used, then

$$d = [(2\pi m + \psi) - \phi + \zeta]\mu$$
$$z = [(2\pi m + \psi) - \phi + \zeta]\lambda + z_0(\eta) - z_0(l)$$

where z_0 is the steady-state displacement of the blade out of the tip path plane and ζ is the spacing between the blade generating the vorticity and the blade at which the downwash is to be computed. For a rigid blade, $z_0(\eta) - z_0(l) = a_0(\eta - l)$.

If a rigid wake is assumed, λ is the mean inflow through the rotor determined from the known thrust and rotor attitude. If nonrigid wake concepts are to be used, then λ is represented by the series

$$\lambda = \lambda_0 + \sum_{n=1}^{\infty} \lambda_{nc} \cos n\phi + \lambda_{ns} \sin n\phi \tag{5}$$

The coefficients λ_n may be approximated, at advance ratios below $\mu = 0.1$, by the various harmonics of inflow at the rotor disk obtained from a first iteration using initially uniform inflow. This is equivalent to assuming that each element of vorticity retains the velocity imparted to it at the rotor disk at the instant it left the blade. More accurately, the coefficients λ_n may be established by using a mean value of inflow experienced by each element in one revolution as it travels rearward under the rotor.

The total downwash due to a single trailing vortex is obtained by integrating Eq. (4) up the wake for each blade. This determines the downwash in terms of the strength Γ of a trailing vortex filament in the wake generated by the change in bound circulation along the blade. In the quasistatic solution, this change may be assumed to occur in n (usually five) increments along the blade and a vortex filament trailed between each increment of strength equal to the change in bound circulation between two adjacent increments. The downwash at the midpoint of each increment can then be expressed in terms of the wake vortex strengths. The bound vortex strength is, in turn, expressed in terms of the downwash and the blade pitch angle. The n resulting simultaneous equations may then be solved for the downwash and loading.

The downwash due to the shed vortex system is

$$dw_2 = -\frac{1}{4\pi R} \times \frac{d\Gamma}{d\phi}\, d\phi\, \frac{A_2 dl}{(A_1^2 + A_2^2 + A_3^2)^{3/2}}$$
$$= F(\phi)d\phi \tag{6}$$

This expression should be integrated with respect to l over each finite interval of the blade before integrating with respect to ϕ [see Eq. (11)].

Analytical solution of the problem would now require the integration of Eqs. (4) and (6) both with respect to ϕ over the wake and with respect to x across the chord in order to obtain the Fourier coefficients of the chordwise vorticity distribution appearing in Eq. (1). These steps are carried out in the Appendix for the simple two-dimensional case in order to clarify the subsequent treatment employed in the solution of the more complicated rotor problem. Evidently, for the rotor in three-dimensions, direct solution of this type is not possible because of the obvious difficulty in solving the resulting integral equation in closed form.

Method of Solution

A combined analytical and numerical procedure will be used to obtain the desired solutions. The rotor wake will be divided up into a "near" wake and a "far" wake, the near wake including that portion attached to the blade and extending approximately one-quarter quadrant from the blade trailing edge.

The chordwise variations in the velocity w induced at the airfoil by the far wake will be neglected. This is equivalent to using lifting-line theory when computing the effects of the far wake on the airfoil bound circulation and lift. If $f(\phi)$ and $F(\phi)$ of Eqs. (4) and (6) are independent of x, then the Fourier coefficients of blade chordwise vorticity are zero

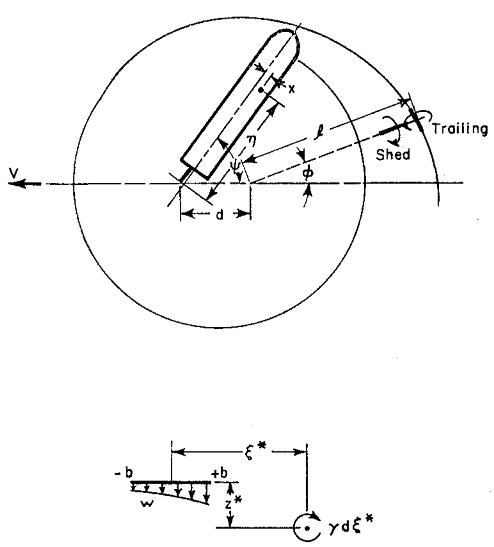

Fig. 3 Geometry of far spiral wake and near straight wake.

except for A_0, whose value for a uniform wake induced downwash w along the blade chord is, from (A5) in the Appendix, $A_0 = -2w$. The bound circulation induced on the blade by w is, therefore, from (A11),

$$\Gamma_b = -2\pi b w \tag{7}$$

and the corresponding lift is, from (A10),

$$L = -2\pi\rho b w V = \rho \Gamma_b V \tag{8}$$

The lifting-line approximation will also be used for the near trailing wake, an approximation that is clearly justified for the high "aspect ratios" of rotors and rotor/propellers. The near shed wake will be treated using analytical techniques and lifting surface theory. In order to examine the validity of this approach, the two-dimensional treatment of the rotor of Ref. 1 will be rederived using a similar treatment of the near and far wake.

Evaluation of Far Wake Lifting-Line Approach for Two-Dimensional Case

In Ref. 1, the effect of the returning wake is determined using a two-dimensional model for the three-dimensional rotor. The far wake is replaced by rows of distributed shed vorticity extending to $\xi = \pm\infty$ below the rotor (Fig. 3) at distances $z = nh$ from the rotor plane in which the near wake is contained. The near wake extends from the trailing edge $\xi = 1$ to infinity. All distances are nondimensionalized in terms of the blade semichord b.

The velocity induced by an element of vorticity $\gamma' d\xi$ in the far wake will now be averaged over the blade chord [Eq. (7)], use made of the results derived in the Appendix for the element of vorticity $\gamma d\xi$ in the near wake, and the integrations performed over both portions of the wake separately. This results in an expression for blade circulation

$$\Gamma_b = \int_1^{\infty} b \left[\frac{\xi + 1}{(\xi^2 - 1)^{1/2}} - 1\right] \gamma d\xi + \sum_{n=1}^{\infty} b \int_{-\infty}^{+\infty} \frac{\xi}{n^2h^2 + \xi^2}\, \gamma' d\xi + \frac{L_q}{\rho V}$$

where L_q is the quasi-static lift, that is, the lift generated in the absence of wake effects. It is shown in the Appendix that the lift may be written in terms of the coefficients of Eq. (1) as

$$dL = b\rho\pi\{\tfrac{1}{2}(\partial/\partial t)(A_0 - \tfrac{1}{2}A_2)b + V(A_0 + \tfrac{1}{2}A_1)\}$$

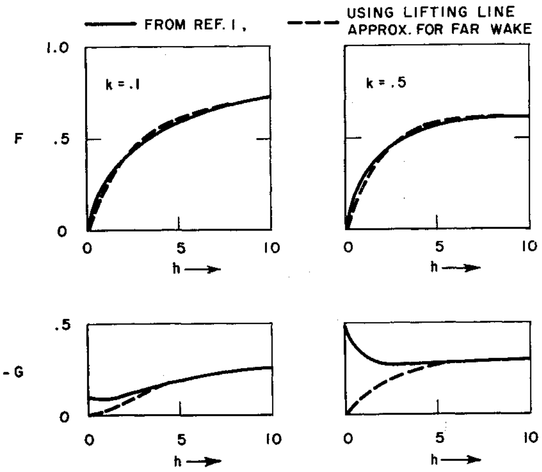

Fig. 4 Comparison between exact and approximate two-dimensional theory.

and again, if the velocity induced over the blade by the far wake is constant over the chord and $\partial\phi/\partial t = 0$, as discussed in the Appendix for the lifting-line approximation, then, after substitution for the coefficients and integration over near and far wake,

$$L = \rho V b \int_1^\infty \frac{\gamma d\xi}{(\xi^2 - 1)^{1/2}} + \rho V b \sum_{n=1}^{\infty} \int_{-\infty}^{+\infty} \frac{\xi}{n^2h^2 + \xi^2}\gamma' d\xi + L_q - \rho\pi \ddot{z} b^2$$

The last term represents the apparent mass or impulsive force. Identifying the shed vorticity with the position of the blade at the time of its shedding, $t - \Delta t$, and assuming a harmonic variation, $\gamma(t) = \gamma_0 e^{i\omega t}$,

$$\gamma(t - \Delta t) = \gamma_0 \exp\{i\omega[t - (b/\Omega R)(\xi - 1)]\}$$

$$\gamma'(t - \Delta t') = \gamma_0 \exp\{i\omega[t - (b/\Omega R)(\xi - 1) - (2\pi n/\Omega)]\}$$

and with $\gamma d\xi^* = -(d\Gamma/dt)dt$ [from Eq. (3)], the lift deficiency function is obtained after manipulations identical to those outlined in the Appendix as

$$C(k,m,h) = \frac{L}{L_q} = \frac{\int_1^\infty \frac{\xi}{(\xi^2-1)^{1/2}} e^{-ik\xi}\, d\xi}{\int_1^\infty \frac{\xi + 1}{(\xi^2 - 1)^{1/2}} e^{-ik\xi}\, d\xi + \sum_{n=1}^{\infty} e^{-2\pi i m} \int_{-\infty}^{+\infty} \frac{\xi}{n^2h^2 + \xi^2} e^{-ik\xi}\, d\xi}$$

where $m = \omega/\Omega$ and $k = \omega b/\Omega R$. The integrals may be evaluated as in Refs. 1 and 17, whence

$$C(k,m,h) = \frac{J_1 - iY_1}{J_1 - iY_1 + Y_0 + iJ_0 + [2i/(e^{hk}e^{2i\pi m} - 1)]}$$

Since the intermediate steps in the foregoing derivation follow the methods of Ref. 1 and the Appendix, only the essential derivations have been included in the preceding very brief outline. The nomenclature is the same as that of Ref. 1, and consequently care should be taken to avoid confusion of the n and m used here (in Ref. 1, n defines the nth wake below the rotor and $m = \omega/\Omega$) with the n and m used elsewhere in this paper, which define the harmonic of rotational speed and the mth wake spiral. For the conditions of harmonic loading, to which the analyses of this paper are confined, $m = \omega/\Omega$ is always an integer; therefore, $e^{2\pi i m} = 1$.

In Fig. 4, a comparison of the exact solution of Ref. 1 with the approximate solution just given is made for the range of reduced frequencies of interest in the present analysis. The real portion of $F(k)$, which establishes the reduction in slope of the lift curve, is closely approximated. At the lower values of h, the error in phase shift, represented by $G(k)$, becomes appreciable. Since the h of interest in rotors is usually above one, this difference does not introduce serious error.

The relative unimportance of the phase shift in determining the magnitude of harmonic loading suggests a further simplification in which the rows of distributed vorticity are replaced by a continuous vortex sheet, an assumption that has a close parallel in the classical vortex theory of the propeller. When the frequency of oscillation ω is now restricted to harmonics of the rotational speed, the vortex strength at any horizontal distance ξ from the airfoil will be the same at all values of z, where z is the vertical distance below the rotor and now replaces nh. The induced velocity at the airfoil due to an element of vorticity in the wake is

$$dw = -\frac{1}{2\pi b}\left[\frac{\xi - x}{z^2 + (\xi - x)^2}\right]\gamma(\xi,z)d\xi^*$$

An infinite spiral sheet implies an infinite number of blades, in which case $x \to 0$ in the foregoing expression. For harmonic loadings, the blade circulation Γ_b will be of the form

$$\Gamma_b = \Gamma_n e^{in\Omega t} \quad \therefore \quad \gamma = \gamma_n e^{in\Omega t}$$

and the element of vorticity in the wake, $\gamma(\xi,z)$, may be identified with the circulation at the time of shedding at time $t - \Delta t$. For any spiral at distance z below the rotor, and using Eq. (3),

$$\gamma(\xi, z)d\xi^* = \gamma(\xi)d\xi^* = -(d/dt)(d\Gamma/dz)dzdt$$

Also,

$$d\xi^*/dt = \Omega R \qquad \Delta t = \xi^*/\Omega R$$

whence

$$\gamma_n(\xi) = -(in/R)(d\Gamma_n/dz)e^{-in\xi^*/R}dz$$

For the "rigid" wake, the spacing between vortex rows h is given by

$$Qhb/2\pi R = \lambda_0 \quad \text{or} \quad h = 2\pi R\lambda_0/Qb$$

where Q is the number of blades. Therefore, in the limit

$$d\Gamma/dz = (Qb/2\pi R\lambda_0)\Gamma_n e^{in\Omega t}$$

Integrating the effect of the entire wake results in an expression for the mean velocity at the airfoil:

$$w = \frac{in\Gamma_n e^{in\Omega t}Q}{4\pi^2 R\lambda_0}\cdot b \int_0^\infty \int_{-\infty}^{+\infty} \frac{e^{inb\xi/R}}{z^2 + \xi^2} d\xi dz$$

The integrals may be evaluated with the help of formula 12, Table 103, Ref. 27, giving the result

$$w = (Q/4\pi\lambda_0 R)\Gamma_n e^{in\Omega t}$$

This is the instantaneous downwash at the blade. Since the airfoil dimension in the x plane has not been considered, the instantaneous lift will be determined only by the quasi-static lift and this induced velocity. Assuming a blade pitch variation of the form $\theta = \theta_n e^{in\Omega t}$, the instantaneous circulation is

$$\Gamma_n = 2\pi\Omega R b\left[\theta_n - \frac{w}{\Omega R}\right] = \frac{2\pi\Omega R b\theta_n}{1 + Qb/2\lambda_0 R}$$

Following the usual definition, the blade solidity σ is given by $\sigma = 2Qb/\pi R$. Since the quasi-static circulation is $\Gamma_q = 2\pi\Omega R b\theta_n$, and the lift, when average downwash velocities over the blade are used, is [Eq. (8)] $L = \rho V\Gamma_b$, it follows that the lift deficiency function now takes the form

$$C = \frac{1}{1 + (\sigma\pi/4\lambda_0)}$$

and is independent of the frequency.

At the lower reduced frequencies, it gives an excellent approximation to the more exact solution, although, by the nature of the analysis, the phase shift cannot be predicted by this method.

An alternate form of the expression C in terms of the wake spacing h is

$$C = \frac{1}{1 + (\pi/h)}$$

and this form has been used to obtain Fig. 5, which shows a comparison with the exact values, replotted from Fig. 4. In view of the excellent agreement between the exact and approximate two-dimensional solutions, it is of interest to attempt a similar analytical solution for the three-dimensional case in vertical flight.

Three-Dimensional Solutions for Vertical Flight

Rotor vortex theory is generally developed on the basis of uniform downwash. This condition is satisfied if the blade has constant circulation along the span, and this, in turn, is satisfied only for the case of ideal twist or taper, that is, varying inversely as the radius. In practice such a condition is closely approximated by the usual linear twist distribution, since the contributions of the blade sections in the region close to the blade root where the ideal twist is clearly not satisfied are small.

Constant circulation implies a tip and center vortex only, with the tip vortex alone contributing to downwash. For this specialized condition, Eq. (4) becomes, for hovering or vertical flight,

$$dw_1 = \frac{\Gamma}{4\pi R}\frac{[1 - \eta\cos(\psi - \phi)]d\phi}{[1 + \eta^2 + z^2 - 2\eta\cos(\psi - \phi)]^{3/2}}$$

The next step involves replacing the spiral of trailing vorticity Γ by a vortex cylinder, which implies an infinite number of blades. The distribution of vorticity along the z axis as developed in the previous section is then

$$d\Gamma/dz = \Gamma Q/2\pi\lambda_0$$

All distances are nondimensionalized in terms of the blade radius R.

The downwash velocity may now be obtained by integration over the complete wake as

$$w_1 = \frac{Q}{8\pi^2\lambda_0 R}\int_0^\infty\int_0^{2\pi}\Gamma \times \frac{[1 - \eta\cos(\psi - \phi)]}{[1 + \eta^2 + z^2 - 2\eta\cos(\psi - \phi)]^{3/2}}d\phi dz$$

$$= \frac{Q}{8\pi^2\lambda_0 R}\int_0^{2\pi}\Gamma\frac{[1 - \eta\cos(\psi - \phi)]}{[1 + \eta^2 - 2\eta\cos(\psi - \phi)]}d\phi$$

$$= \frac{Q}{8\pi^2\lambda_0 R}\int_0^{2\pi}\Gamma[1 + \eta\cos(\psi - \phi) + \eta^2\cos 2(\psi - \phi) + \ldots]d\phi \qquad \eta < 1$$

Considering first the simple case of constant thrust, and hence Γ constant, this results in

$$w = \Gamma Q/4\pi\lambda_0 R$$

independent of η. Since $\lambda_0 = w/\Omega R$ in hovering flight,

$$\Gamma = 4\pi\lambda_0{}^2\Omega R^2/Q$$

The total rotor thrust is

$$T = QR^2\int_0^1 \rho\Omega\eta\Gamma d\eta = 2\rho\pi R^2\cdot\Omega^2R^2\cdot\lambda_0{}^2$$

or, with the definition $C_T = T/\rho\pi R^2\Omega^2R^2$,

$$\lambda_0 = (C_T/2)^{1/2}$$

as in actuator disk theory.

Considering next the case when Γ varies harmonically with azimuth such that

$$\Gamma_n = \Gamma_{ns}\sin n\phi + \Gamma_{nc}\cos n\phi$$

then

$$w_1 = \frac{\Gamma_{ns}Q}{8\pi^2\lambda_0 R}\pi\eta^n\sin n\psi + \frac{\Gamma_{nc}Q}{8\pi^2\lambda_0 R}\pi\eta^n\cos n\psi$$

The downwash thus has the same periodicity as the circulation change, and the spanwise distributions are increasingly concentrated at the tip as the order of the harmonic increases, a result somewhat similar to that obtained in Ref. 5. However, a complete solution requires the introduction of the contributions of the shed vorticity. From Eq. (6) specialized for hovering, the total downwash due to the shed vorticity is

$$w_2 = \int_0^\infty\int_0^{2\pi}\int_0^1 \frac{d}{dz}\frac{d\Gamma}{d\phi}d\phi\frac{1}{4\pi R} \times \frac{\eta\sin(\psi - \phi)}{[\eta^2 + l^2 + z^2 - 2\eta l\cos(\psi - \phi)]^{3/2}}dldz$$

The order of integration may be interchanged, since the singularities are retained in either process. After integrating with respect to z and expanding in a sine series,

$$w_2 = \frac{Q}{8\pi^2\lambda_0 R}\int_0^{2\pi}\int_0^\eta \frac{d\Gamma}{d\phi}d\phi \times \left[\frac{1}{\eta}\sin(\psi - \phi) + \frac{l}{\eta^2}\sin 2(\psi - \phi) + \ldots\right]dl + \frac{Q}{8\pi^2\lambda_0 R}\int_0^{2\pi}\int_\eta^1 \frac{d\Gamma}{d\phi}d\phi \times \left[\frac{\eta}{l^2}\sin(\psi - \phi) + \frac{\eta^2}{l^3}\sin 2(\psi - \phi) + \ldots\right]dl$$

which reduces, after substituting $\Gamma = \Gamma_{ns}\sin n\phi + \Gamma_{nc}\cos n\phi$ and integrating over ϕ and l, to

$$w_2 = \frac{Q}{8\pi^2\lambda R}[\Gamma_{ns}(2 - \eta^n)\pi\sin n\psi + \Gamma_{nc}(2 - \eta^n)\pi\cos n\psi]$$

Summing the downwash due to the trailing and shed vorticity leads to the interesting result

$$w = (Q/4\pi\lambda_0 R)[\Gamma_{ns}\sin n\psi + \Gamma_{nc}\cos n\psi]$$

This is the same result as was obtained in the previous section

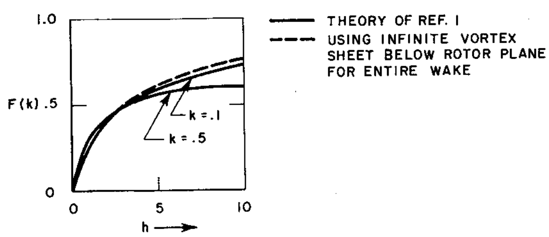

Fig. 5 Effect of assuming an infinite number of blades in two-dimensional solution.

for the two-dimensional case and, in a similar manner, results in a lift deficiency function

$$C = 1/[1 + (\sigma\pi/4\lambda_0)]$$

A more general solution may be obtained for the case where the circulation on the blade is expressed as a power series:

$$\Gamma_b(l) = 2\pi b\Omega R \sum_{r=0}^{\infty} \gamma_r l^r$$

Solutions to this case may be more readily obtained if the periodicity of the circulation is expressed in complex form $\Gamma = \Gamma_n e^{in\phi}$. Furthermore, it will be assumed that the mean downwash through the rotor is initially uniform over the disk.

The trailing vortex system will now consist of the tip vortex, whose value is

$$\Gamma(1) = 2\pi b\Omega R \sum_{r=0}^{\infty} \gamma_r$$

and a sheet of trailing vorticity due to the change in circulation $-d\Gamma_b/dl$ along the span. The downwash due to this sheet of vorticity is given by Eq. (4) specialized for the hovering case. The total downwash is obtained by integration over the complete wake:

$$w_1(\psi,\eta) = -\frac{1}{4\pi R}\int_0^\infty\int_0^1\int_0^{2\pi}\frac{d}{dl}\frac{d\Gamma}{dz}\times \frac{[l-\eta\cos(\psi-\phi)]l}{[l^2+z^2+\eta^2-2\eta l\cos(\psi-\phi)]^{3/2}}\,d\phi\,dl\,dz$$

which, after integration with respect to z, results in

$$w_1(\psi,\eta) = -\frac{1}{4\pi R}\int_0^\eta\int_0^{2\pi}\frac{d}{dl}\frac{d\Gamma}{dz}\frac{l}{\eta}\times \frac{[l/\eta-\cos(\psi-\phi)]}{[(l/\eta)^2+1-2(l/\eta)\cos(\psi-\phi)]}\,d\phi\,dl - \frac{1}{4\pi R}\int_\eta^1\int_0^{2\pi}\frac{d}{dl}\frac{d\Gamma}{dz}\frac{[1-\eta/l\cos(\psi-\phi)]}{[1+(\eta/l)^2-2\eta/l\cos(\psi-\phi)]}\,d\phi\,dl$$

The first integral gives the downwash in the rotor plane outside a vortex cylinder extending to infinity from the rotor plane and is zero for Γ_0. This, however, is not the case when Γ varies with time (azimuth), and the independence of blade elements is not, therefore, as readily proved for this case.

Integration with respect to ϕ may be performed, when Γ has the form $\Gamma_n e^{in\phi}$, by change of variable, $y = e^{i(\psi-\phi)}$, and application of the theorem of residues. The result is

$$w_1 = \frac{Qe^{in\psi}}{8\pi^2\lambda_0 R}\left[\pi\int_0^\eta \frac{d}{dl}\Gamma_n(l)\left(\frac{l}{\eta}\right)^n dl - \pi\int_\eta^1\frac{d}{dl}\Gamma_n(l)\left(\frac{\eta}{l}\right)^n dl\right]$$

Similarly, the contribution of the shed wake may be obtained as

$$w_2 = \frac{Qe^{in\psi}}{8\pi^2\lambda_0 R}\left[n\pi\int_0^\eta \Gamma_n(l)\frac{l^{n-1}}{\eta}\,dl + n\pi\int_\eta^1\Gamma_n(l)\frac{\eta^n}{l^{n-1}}\,dl\right]$$

To these must be added the contribution of the tip vortex:

$$w_1 = (Qe^{in\psi}/8\pi^2\lambda_0 R)\pi\Gamma(1)$$

With $\Gamma_n = 2\pi b\Omega R\Sigma\gamma_r l^r$, the integrals may be evaluated by integrating term by term ($l < 1$). The result is, for the nth harmonic of downwash,

$$\lambda_n = \frac{\sigma}{8\lambda_0}\left[2\pi\sum_0^\infty\gamma_r\eta^r\right] = \frac{\sigma\pi}{4\lambda_0}\sum_0^\infty\gamma_r\eta^r$$

The downwash at η thus depends only on the circulation at η, and the lift deficiency function is the same as that previously obtained. For example, if the variation in downwash $\gamma_r\eta^r$ is obtained by a pitch variation of the form $\theta = \theta_{n_r}\eta^r$, then the instantaneous circulation is

$$\Gamma_n = 2\pi\Omega rb[\theta_{n_r}\eta^r - (\lambda_n/\eta)]$$

or, since l and η are interchangeable variables,

$$\sum_{r=0}^\infty\gamma_r\eta^r = \theta_{n_r}\eta^{r+1} - \frac{\sigma\pi}{4\lambda_0}\sum_0^\infty\gamma_r\eta^r$$

and $\gamma_r/\theta_{n_r} = 1/[1 + (\sigma\pi/4\lambda_0)]$ as before.

This reduction in circulation due to the wake is of particular importance when it is desired to use a rigid or semirigid propeller as a control device by use of a first harmonic cyclic pitch variation. Since small stiff propellers suggest high disk loadings, C_T will be high or, alternatively, downwash λ_0 is high, and appreciable reductions in moment over those predicted by quasi-static aerodynamics will result.

For example, consider a rotor/propeller with a disk loading of 25 psf, a tip speed of $\Omega R = 700$ fps, and operating at a mean angle of attack of $a_T = 0.1$ rad. Then $C_T = 25/\rho\Omega^2R^2 = 0.0214$ and $C = 0.49$, resulting in about half the moment predicted by simple blade element theory. Evidently, a similar result will occur following rapid increase of collective pitch of a control rotor, resulting in a lag in thrust which may become of importance if high-gain automatic stabilization equipment is installed.

The preceding analysis has been developed with the usual assumption of a rigid wake. The effect of this assumption may be seen by deriving the same result from consideration of simple momentum and blade element theory.

From momentum theory, for uniform steady inflow and a superimposed periodic thrust change, $T_n e^{in\Omega t} = 2 \times$ mass flow through rotor $\times\, w_n e^{in\Omega t}$, where w_n is the velocity change through the rotor disk due to T_n.

Considering mean velocity only, $w_0 = \lambda_0\Omega R$, in determining the mass flow,

$$T_n = 2\times\rho\pi R^2\times\lambda_0\Omega R\times\lambda_n\Omega R \text{ or } C_T = 2\lambda_0\lambda_n$$

From the blade element theory for uniform flow through the rotor and periodic change in pitch, $\theta_n e^{in\Omega t}$,

$$C_{T_n}e^{in\Omega t} = (\sigma\pi/2)(\theta_n - \lambda_n)e^{in\Omega t}$$

and with $C_{T_{qn}} = (\sigma\pi/2)\theta_n$, $C_{T_n}/C_{T_{qn}} = 1/[1 + (\sigma\pi/4\lambda_0)]$, as in the vortex theory.

If, on the other hand, the periodic thrust were to be computed using the nonrigid wake concept of vortex theory [Eq. (4)], then λ_n would have to be included in the computation of mass flow.

Three-Dimensional Solutions in Forward Flight

Near Shed Wake: $\Gamma_N{}^S$

Having established the validity of the proposed approach and obtained an analytical solution for the limiting case of vertical flight, it is possible to proceed with some confidence to the solution for the three-dimensional rotor in forward flight. The treatment of the near wake will be considered first, and in particular the near shed wake, since this wake introduces the important singularities of classical unsteady aerodynamic theory. The method of solution presented in the Appendix may be followed directly if the curvature of the wake is neglected as in Ref. 14 and, furthermore, if the blade is treated as a two-dimensional airfoil in the presence of an element of vorticity $\gamma d\xi^*$ at ξ^* from the origin. The considerable simplification in the analysis resulting from the latter assumption appears justified on the basis of the results of Ref. 14, in which close agreement was obtained between the two-dimensional and three-dimensional solutions. This approximation is clearly inadmissible when treating the far wake.

The circulation due to the near wake may then be determined by assuming the straight near wake to extend aft of the blade to infinity. Following the treatment in the Appendix and integrating over the near wake for all vortex elements results in an expression for the bound circulation on the blade due to the near shed wake:

$$\Gamma_N{}^S = \int_1^\infty b\gamma(\xi)\left[\frac{\xi+1}{(\xi^2-1)^{1/2}} - 1\right]d\xi$$

To this must be added the circulation due to the far wake. Additional circulation arises from the velocity u of Eq. (2), which will be designated as the quasi-static circulation $\Gamma_q = -2\pi bu$.

For a symmetrical blade spacing and when the frequency of oscillation is an integer of rotational speed, the effects on one blade of the bound vortices from the remaining blades are zero for the case of Γ_0 and when n is equal to or a multiple of the number of blades. This is not otherwise true. However, unless a very large number of wide chord blades are used, the effects of the bound vortices on each other are negligible and may be ignored. This may be readily verified from Eq. (6), as discussed in determining the choice of upper limit in the integral (11).

Since we are concerned here with harmonic blade loads and motions, the blade bound circulation Γ_b will be defined as

$$\Gamma_b(\psi) = \sum_{n=0}^{\infty} \Gamma\eta_{ns_l}\sin n\Omega t + \Gamma_{nc_l}\cos n\Omega t \qquad (9)$$

$$dw_2(\psi,\phi) = -\frac{1}{4\pi R}\left\{\frac{\eta\sin(\psi-\phi)+d\sin\phi}{z^2+[\eta\sin(\psi-\phi)+d\sin\phi]^2}\left[\frac{l+d\cos\phi-\eta\cos(\psi-\phi)}{[l^2+\eta^2+z^2+d^2-2\eta l\cos(\psi-\phi)+2dl(\cos\phi-\eta\cos\psi)]^{1/2}} - \frac{d\cos\phi-\eta\cos(\psi-\phi)}{[\eta^2+z^2+d^2-2\eta d\cos\psi]^{1/2}}\right]\right\}\frac{d\Gamma}{d\phi}d\phi = -\frac{1}{4\pi R}g(\phi)\frac{d\Gamma}{d\phi}d\phi \qquad (11)$$

where the trigonometric rather than the complex form is employed in keeping with the more usual practice in rotary wing aerodynamics.

The distortion of the near shed wake vorticity distribution due to the first harmonic variations of forward velocity will be neglected, and hence the relationship for velocity is $d\xi^*/dt = \Omega\eta R$. The shed vorticity in the wake may be related to the time rate of change of blade circulation [Eq. (3)] as

$$\gamma(\xi)d\xi^* = -(d/dt)\Gamma_b dr$$

whence, since Ω is constant,

$$\gamma(\xi) = -\frac{1}{\Omega\eta R}\frac{d}{dr}\Gamma_b = -\frac{n}{\eta R}\sum_0^\infty \Gamma_{ns_l}\cos n\Omega t - \Gamma_{nc_l}\sin n\Omega t$$

An element of shed vorticity in the wake may then be identified with the position of the blade trailing edge b at the time of its shedding, $t - \Delta t$. Now $t = \psi/\Omega$, and $\Delta t = (\xi^* - b)/\Omega\eta R$; therefore,

$$\gamma(\xi) = \sum_{n=0}^{\infty} -\frac{n}{\eta R}\left\{\Gamma_{ns_l}\cos n\left[\psi - \frac{b}{\eta R}(\xi-1)\right] - \Gamma_{nc_l}\sin n\left[\psi - \frac{b}{\eta R}(\xi-1)\right]\right\}$$

Substituting in the integral for $\Gamma_N{}^S$ results in

$$\Gamma_N{}^S(\psi) = -\frac{nb}{\eta R}\{[\Gamma_{ns_l}\cos n\psi - \Gamma_{nc_l}\sin n\psi]I_c - [\Gamma_{ns_l}\sin n\psi + \Gamma_{nc_l}\cos n\psi]I_s\} \qquad (10)$$

where

$$I_c = \int_1^\infty \cos\frac{nb}{\eta R}(\xi-1)\left[\frac{\xi+1}{(\xi^2-1)^{1/2}} - 1\right]d\xi$$

$$I_s = \int_1^\infty \sin\frac{nb}{\eta R}(\xi-1)\left[\frac{\xi+1}{(\xi^2-1)^{1/2}} - 1\right]d\xi$$

The coefficient $nb/\eta R$ appearing in the solution is the well-known reduced frequency k specialized to the case of the nth harmonic of rotational speed at the blade station η in question. The integrals, first computed numerically in Ref. 21, may be identified[17] as

$$I_c = (\pi/2)(Y_0 + J_1)\cos k - (\pi/2)(Y_1 - J_0)\sin k$$

$$I_s = (\pi/2)(Y_0 + J_1)\sin k - (\pi/2)(Y_1 - J_0)\cos k - (1/k)$$

Far Shed Wake: $\Gamma_F{}^S$

The far shed wake will be treated by neglecting the chordwise variation of velocity along the airfoil chord due to the wake. Since the primary effect of the wake appears as the blade passed over the shed or trailing vortex line generated by itself or by another blade, and since the distance of these vortex lines below the blade may be of the order of one chord length, the validity of the assumption may well be questioned. However, the analysis of the equivalent assumption for the two-dimensional case just given for comparison with the exact solution obtained in Ref. 1 indicates that the assumption is certainly valid, at least for the reduced frequencies of interest in rotor blade loading analysis.

Setting x and χ equal to zero in line with the preceding assumption, it is possible to perform the integration of Eq. (6) with respect to l for the case where λ is constant and to obtain the contribution of a vortex line extending from 0 to l. This integration may be performed with the aid of formula 167 of Ref. 26, giving the result

The total downwash at the blade at any station η and azimuth position ψ is obtained by integration over the far wake over m spirals:

$$w_2 = -\int_{\psi+\zeta}^{2\pi m+\psi+\zeta-(\pi/2)} \frac{1}{4\pi R}g(\phi)\frac{d\Gamma}{d\phi}d\phi$$

The choice of the upper limit in the integration must be made with some care. Defining the end of the far wake at an azimuth angle $\pi/2$ from the blade appears to be reasonable, and little error is involved if this angle is varied from $\pi/2$ to $3\pi/2$ or decreased to $\pi/4$. Evidently, this choice must be made on the basis of blade and rotor geometry; however, a simple integration of Eq. (6) for the case $z = d = 0$ and $\psi - \phi$ varying from 0 to $\pi/2$ or greater will generally clearly indicate the desirable choice of upper limit.

As in the case of the near wake, elements of vorticity in the far wake are identified with the position of the blade at the instant of their shedding and in terms of the time rate of change of bound circulation, whence, from (9),

$$\frac{d\Gamma}{d\phi} = \sum_{n=0}^{\infty} -n\,[\Gamma_{ns_l}\cos n\phi - \Gamma_{nc_l}\sin n\phi]$$

When the bound circulation varies appreciably over the span, the actual circulation may be represented by a series of straight distributions extending from zero to various spanwise locations l.

Substituting in the integral for w_2,

$$w_2 = \sum_l \sum_{n=0}^{\infty} \frac{n}{4\pi R}\int_{\psi+\zeta}^{2\pi m+\psi+\zeta-\pi/2} [\Gamma_{ns_l}\cos n\phi - \Gamma_{nc_l}\sin n\phi]g(\phi)d\phi$$

which may be written in the form

$$w_2 = \sum_l \sum_{n=0}^{\infty} \frac{n}{4\pi R}\sum_{k=0}^{\infty} [\Gamma_{ns_l}(A_{nc_l}{}^k\cos k\psi + B_{nc_l}{}^k\sin k\psi) - \Gamma_{nc_l}(A_{ns_l}{}^k\cos k\psi + B_{ns_l}{}^k\sin k\psi)] \qquad (12)$$

where the coefficients A and B are obtained from harmonic analysis with respect to ψ of the results of numerical evaluation of the integral over the wake for m spirals at values of ψ from 0° to 360°. A_{ncl}^k identifies the cosine coefficient of the kth harmonic due to a cos$n$ variation of bound circulation extending from 0 to l, and similarly with the remaining coefficients.

Trailing Wake: Γ^T

A treatment for the system of trailing vortices using Eq. (4) similar to that used for the far shed wake results in

$$w_1 = \sum_l \sum_{n=0}^{\infty} \frac{1}{4\pi R} \int_{\psi+\zeta}^{2\pi m+\psi+\zeta} [\Gamma_{ns_l} \sin n\Omega t + \Gamma_{nc} \cos n\Omega t] f(\phi,\psi)$$

whence

$$w_1 = \sum_l \sum_{n=0}^{\infty} \frac{1}{4\pi R} \sum_{k=0}^{\infty} [\Gamma_{ns}(P_{nsl}^k \cos k\psi + Q_{nsl}^k \sin k\psi) + \Gamma_{ncl}(P_{ncl}^k \cos k\psi + Q_{ncl}^k \sin k\psi)] \quad (13)$$

where l now identifies the spanwise blade station from which the trailing vortex is assumed to originate.

Determination of Blade Circulation and Lift

Substituting the expressions for w_1 and w_2 in (7) results in an expression for the bound circulation on the blade induced by a wake generated by changes in this bound circulation. The total bound circulation on the blade may now be obtained as

$$\Gamma_b = \Gamma_N{}^S + \Gamma_F{}^S + \Gamma^T + \Gamma_q \quad (14)$$

where Γ_q is the quasi-static circulation, previously defined as that which would occur in the absence of any wake effects.

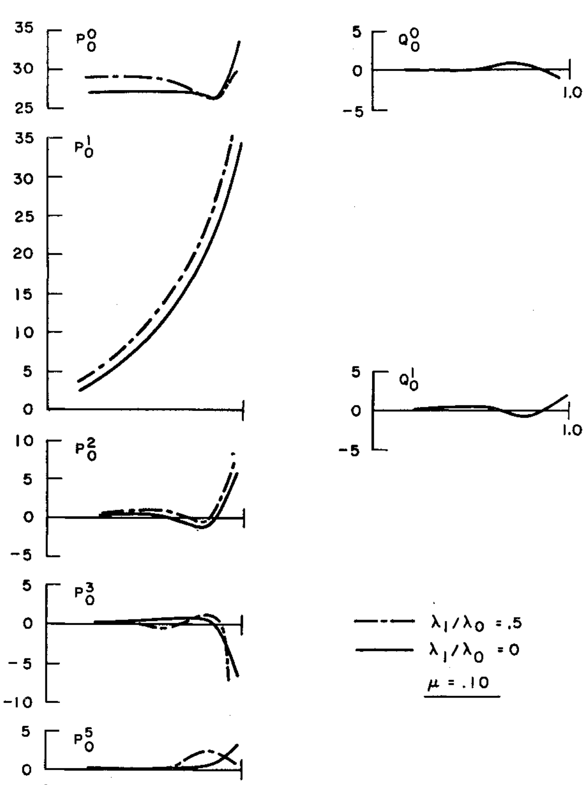

Fig. 6 Spanwise distribution of harmonic downwash coefficients at blade due to wake of constant strength, $n = 0$. Transition flight regime.

In order to obtain Γ_q, it is necessary to define the blade motion. This motion may consist of contributions from all of the blade normal modes, and in cases where the blade is operating close to resonance the dominant mode should be included. For the purpose of illustration, a rigid nontwisting blade flapping through the angle β will be used operating at a pitch setting $\theta(\eta)$, which includes the built-in twist. Then u is uniform over the blade chord and is given by

$$u = -\Omega R[(\eta + \mu \sin\psi)\theta(\eta) - (\eta\dot{\beta} + \mu\beta \cos\psi)]$$

From (7), it follows that $\Gamma_q = 2\pi bu$. The contribution of the near shed wake is given by Eq. (10), which may be written in the form

$$\Gamma_N{}^S = -\sum_{n=1}^{\infty} (\Gamma_{ns}C_n + \Gamma_{nc}S_n) \cos n\psi + (\Gamma_{ns}S_n - \Gamma_{nc}C_n) \sin n\psi$$

where $C_n = I_c k$, $S_n = I_s k$, and $k = nb/\eta R$.

The contributions of the far shed wake and trailing wake may be expressed in terms of the total downwash normal to the tip path plane expressed nondimensionally as

$$\lambda = [(w_1 + w_2)/\Omega R] - \mu \tan i \quad (15)$$

where w_2 now contains only the far shed wake and i is the angle between the tip path plane and the relative wind, positive nose up. Then, from Eq. (7),

$$\Gamma^T + \Gamma_F{}^S = -2\pi b \Omega R \lambda$$

If the flapping angle β is expressed as

$$\beta = a_0 - \sum_{n=1}^{\infty} a_n \cos n\psi + b_n \sin n\psi$$

and the bound circulation and inflow λ are defined in the series form given by Eqs. (9) and (5), then equating coefficients in Eq. (14) results in an expression for Γ_n. At this point, a nondimensional form of the circulation will be introduced and defined as

$$\gamma_n = \Gamma_n / 2\pi b \Omega R$$

Then, in nondimensional form,

$$\left.\begin{aligned}
\gamma_0 &= [\eta\theta - \lambda_0 - (\mu/2)a_1] \\
\gamma_{1s} &= [\mu\theta - \lambda_{1s} - a_1\eta + (\mu/2)b_2] - (\gamma_{1s}S_1 - \gamma_{1c}C_1) \\
\gamma_{1c} &= [-\lambda_{1s} + b_1\eta - a_0\mu + (\mu/2)a_2] - (\gamma_{1s}C_1 + \gamma_{1c}S_1) \\
\gamma_{ns} &= [-\lambda_{ns} - n\eta a_n + (\mu/2)(b_{n+1} + b_{n-1})] - (\gamma_{ns}S_n - \gamma_{nc}C_n) \\
\gamma_{nc} &= [-\lambda_{nc} + n\eta b_n + (\mu/2)(a_{n+1} + a_{n-1})] - (\gamma_{ns}C_n + \gamma_{nc}S_n)
\end{aligned}\right\} \quad (16)$$

The lift, after summing over the entire wake, may be obtained separately, for the near wake, from (A12) in the Appendix and, for the far wake, from (8) in the form

$$L(\eta) = \rho V b \int [\gamma d\xi/(\xi^2 - 1)^{1/2}] + \rho V(\Gamma^T + \Gamma_F{}^S + \Gamma_q) + \rho\pi\ddot{z}b^2$$

which, after the identification of $\gamma(\xi)$ with the blade position at the time of its shedding, as was done for the circulation, becomes

$$L(\eta) = -(nb/\eta R)\rho V[\Gamma_{ns} \cos n\psi - \Gamma_{nc} \sin n\psi]I_c' - (nb/\eta R)\rho V[\Gamma_{ns} \sin n\psi + \Gamma_{nc} \cos n\psi]I_s' + \rho V[\Gamma^T + \Gamma_F{}^S + \Gamma_q] + \rho\pi\ddot{z}b^2 \quad (17)$$

where, with $k = nb/\eta R$ as before,

$$I_s' = \int_1^\infty \sin\frac{nb}{\eta R}(\xi - 1)\frac{d\xi}{(\xi^2-1)^{1/2}} = \frac{\pi}{2}J_0\cos k + \frac{\pi}{2}Y_0\sin k$$

and

$$I_c' = \int_1^\infty \cos\frac{nb}{\eta R}(\xi - 1)\frac{d\xi}{(\xi^2-1)^{1/2}} = \frac{\pi}{2}J_0\sin k - \frac{\pi}{2}Y_0\cos k$$

That Eq. (16) reduces to the classical case for a two-dimensional airfoil may be readily verified by letting $\Gamma^T = \Gamma_F{}^S = 0$ and expressing the circulation in complex form:

$$\Gamma = \Gamma_n e^{in\psi} \qquad \Gamma_q = \Gamma_{q_n} e^{in\psi}$$

Then, with $\Gamma_{nc} = \Gamma_n$, $\Gamma_{ns} = i\Gamma_n$, we obtain from (10) and (14)

$$\Gamma_n = -ik\Gamma_n[I_c - iI_s] + \Gamma_{q_n} = -ik\Gamma_n\left[\int_1^\infty e^{ik(1-\xi)}\frac{\xi+1}{(\xi^2-1)^{1/2}}d\xi - e^{ik}\int_1^\infty e^{-ik\xi}d\xi\right] + \Gamma_{q_n}$$

or

$$\Gamma_n = \Gamma_{q_n}\Big/ ike^{ik}\int_1^\infty e^{-ik\xi}\frac{\xi+1}{(\xi^2-1)^{1/2}}d\xi$$

Similarly, with $L = L_n e^{in\Omega t}$ from (17),

$$L_n = -ik\rho V\Gamma_n[I_c' - iI_s'] + L_{q_n} + \rho\pi\ddot{z}b^2 = -ik\rho V\Gamma_n e^{ik}\int_1^\infty \frac{e^{-ik\xi}}{(\xi^2-1)^{1/2}}d\xi + L_{q_n} + \rho\pi\ddot{z}b^2$$

Since $L_{q_n} = \rho V\Gamma_{q_n}$, it follows that

$$L_n = L_{q_n}\left[\int_1^\infty \frac{\xi e^{-ik\xi}}{(\xi^2-1)^{1/2}}d\xi \div \int_1^\infty \frac{(\xi+1)e^{-ik\xi}}{(\xi^2-1)^{1/2}}d\xi\right] + \pi\rho\ddot{z}b^2$$

The coefficient of L_{q_n} may be readily identified as the lift deficiency function $C(k)$ of Ref. 17.

Blade Flapping Coefficients

The blade displacements are obtained from the blade flapping equilibrium equation

$$I\Omega^2\left(\frac{\ddot{\beta}}{\Omega^2} + \beta\right) = R^2\int_0^1 \eta L(\eta)d\eta$$

where the flapping hinge offset has been assumed to be substantially zero. The effect of the offset is not large unless the blade Lock number is low and the offset appreciable. The coefficients a_n, b_n decrease rapidly as n increases, and consequently the lift may be approximated for the purpose of determining a_n, b_n by its quasi-static value [Eq. (8)]

$$L(\eta) = \rho V\Gamma_0(\eta)$$

or

$$I\Omega^2\left(\frac{\ddot{\beta}}{\Omega^2} + \beta\right) = 2\pi\rho bR^4\Omega^2\int_0^1 (\eta + \mu\sin\psi) \times \left[\gamma_0 + \sum_{n=1}^{\infty}\gamma_{ns}\sin n\psi + \gamma_{nc}\cos n\psi\right]\eta\, d\eta$$

The mass constant or Lock number of the rotor blade is

$$LN = 2\rho\pi bR^4/I$$

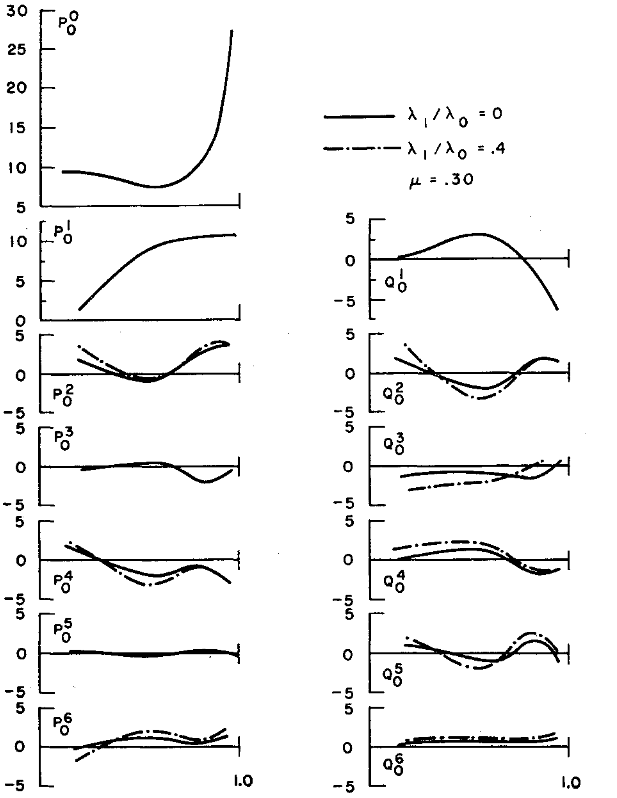

Fig. 7 Spanwise distribution of harmonic downwash coefficients at blade due to wake of constant strength, $n = 0$. Cruise flight regime.

where the designation LN is used in place of the more usual γ in order to avoid confusion with the circulation.

After solution of the differential equation for the particular integral representing steady-state flapping motion, the coefficients of the Fourier series for blade motion are obtained as

$$\left.\begin{aligned} a_n &= \frac{LN}{2(n^2-1)}\int_0^1\left\{\eta^2\gamma_{nc} + \frac{\mu}{2}\eta[\gamma_{(n+1)s} - \gamma_{(n-1)s}]\right\}d\eta \\ b_n &= \frac{LN}{2(n^2-1)}\int_0^1\left\{\eta^2\gamma_{ns} + \frac{\mu}{2}\eta[\gamma_{(n-1)c} - \gamma_{(n+1)c}]\right\}d\eta \end{aligned}\right\} \quad (18)$$

All relationships necessary for the determination of the blading loading have now been established.

Numerical Results: Transition Flight Regime

In order to examine the nature of the induced flow through the rotor in forward flight, Eqs. (4, 6, and 11) were programed for numerical integration on high-speed digital computers (IBM 709 and 7090). Such solutions are, of course, specialized, but several general conclusions can be drawn from the results, and the feasibility of computing air loads by the method just described can be determined.

Before proceeding with the complete solutions, several trial runs were made to determine the number m of spirals and intervals in both ϕ and ψ required for an accurate prediction of the harmonic content of the wake up to at least the sixth harmonic. The number of spirals was varied from $m = 3$ to $m = 12$ and the interval sizes from $\Delta\phi = \Delta\psi = 2.5°$ to 20°. A satisfactory compromise was found to be three spirals and intervals of 7.5° in the far wake and 2.5° in the near wake, giving a solution time on the 7090 computer of approximately 0.5 min for the downwash at one spanwise location due to one blade wake and for one harmonic.

In Figs. 6 and 7 is plotted the harmonic content, up to the sixth harmonic, of the downwash at the rotor generated by a tip vortex of constant strength for two values of μ corresponding to transition and to cruise flight regimes. Unlike the fixed wing, a rotor blade is highly loaded at the tip, and many of the basic characteristics of the downwash may, therefore, be determined by examining the effects of the powerful system of trailing vortices shed over the outer few percent of the blade span, a system adequately represented by a single tip vortex of strength equal to the mean blade circulation.

Considering first the transition case $\mu = 0.1$, it is evident from Fig. 6 that the steady-state value of downwash is substantially constant over the disk and that the initial assumption of constant Γ_0 is satisfied. Of considerable interest is the pronounced first harmonic variation in downwash generated by the tip vortex which, at low advance ratios, will produce an upwash at the leading edge. The existence of this first harmonic variation in downwash was first predicted by the theory of Ref. 4 and demonstrated by the flight test observations in Ref. 22 and the wind-tunnel tests of Ref. 23. In forward flight, the spiral formed by the tip vortex is displaced aft, and, since the velocity field outside the spiral has a vertical component, all points ahead will experience an upwash. Evidently, the assumption of uniform inflow is violated, and a further cycle is necessary before the downwash can be defined with any accuracy. Before this can be done, it is necessary to relate the downwash characteristics to a particular flight condition and rotor configuration, in particular, to the total inflow through the rotor. This not only consists of the downwash, that is, the velocities induced at the rotor disk by the wake, but also contains components of the forward and climbing velocities. Although the curves of Fig. 6 are specialized to a particular total inflow of $\lambda_0 = 0.05$, to a three-bladed rotor, and to a forward flight of $\mu = 0.10$, they are otherwise generalized and will fit a wide variation of rotor attitudes, thrust coefficients, and solidities.

Since the wake is generated by the blades, the inflows that have been computed are those relative to a particular blade, and, if, the higher harmonic motions of the blade above the first are ignored, a valid assumption and certainly well within the limitations of the assumed wake geometry, then the inflows plotted are those perpendicular to the plane containing the blade tips or the tip path plane. The steady-state values of λ and μ which appear in the solutions should therefore be computed on this basis. It should be noted that the bulk of published rotor information uses the control axis as reference; however, the conversion from one system to another involves only minor corrections and is readily made. For a discussion of the different reference axes, see Ref. 28.

The induced flow w is directly proportional to the strength of the tip vortex. The steady-state component due to a steady state tip vortex Γ_0 is, from Eq. (13),

$$w_1/\Omega R = \lambda_{0i} = (b/2R)\gamma_0 P_0^0$$

Hence, from Eq. (15), the total inflow is

$$\lambda_0 = (b/2R)\gamma_0 P_0^0 - \mu \tan i$$

Now P_0^0 is a function only of λ_0 and the number of blades used; consequently, the numerical integrations from which P_0^0 is obtained may be used to represent any desired combination of rotor solidity, represented by b/R, and circulation γ_0, determined in turn by the collective pitch setting θ.

For example, consider a helicopter climbing out at an angle of incidence of $i \simeq -15°$ or, alternatively, accelerating through transition with this tip path plane inclination. These would be typical operational flight regimes at advance ratios of the order of $\mu = 0.1$. The induced flow is, then, for λ_0 of 0.05,

$$\lambda_{0i} = \lambda_0 + \mu \tan i = 0.023$$

The corresponding rotor thrust coefficient is, for constant bound circulation,

$$C_T = (\sigma\pi/2)\gamma_0$$

The rotor configuration must now be defined. Selecting a solidity of $\sigma = 0.07$ defines $b/2R = 0.0183$. From Fig. 6, the mean steady downwash coefficient is $P_0^0 \simeq 28$, whence

$$\gamma_0 = (\lambda_{0i}/P_0^0)\cdot(2R/b) = 0.045 \qquad \text{and} \qquad C_T = 0.00495$$

Using the approximate momentum relations for forward flight suggested by Glauert would give

$$C_T = 2(\lambda_0 + \mu \tan i)(\lambda_0^2 + \mu^2)^{1/2} = 0.005$$

and evidently this approximate relationship is in good agreement with the vortex theory developed in this paper.

A correction will now be introduced in the numerical solutions for the first harmonic variation in downwash. The tip vortex will be assumed to descend with the steady and first harmonic inflows occurring at a representative tip station; z in Eq. (4) must then be multiplied by $\lambda_0 + \lambda_1 \cos\phi$ or by

$$\lambda_0\left[1 + \frac{P_0^1}{P_0^0}\left(1 + \frac{\mu \tan i}{\lambda_0}\right)\cos\phi\right]$$

instead of simply λ_0. For the conditions selected, and using P_0^1/P_0^0 of 1.12 from Fig. 6, the result is

$$\frac{\lambda_1}{\lambda_0} = \frac{P_0^1}{P_0^0}\left(1 + \frac{\mu \tan i}{\lambda_0}\right) \simeq 0.5$$

The effect of introducing this correction is indicated in Fig. 6.

If, instead of accelerating or climbing out through transition, a helicopter is required to maintain steady flight in this regime, then an interesting and highly significant phenomenon occurs which may be described as a tendency for the rotor to suck up its own wake into the leading edge of the tip path plane. Evidently, if i is small or even positive as would occur in a flare, then the ratio λ_1/λ_0 may approach or exceed unity, and the blades will pass through their own wake. When this occurs, large higher harmonic components in inflow can be computed, indicating large local variations in angle of attack. Such computations are, however, quantitatively meaningless, since all of the basic assumptions of the mathematical model employed are violated. For example, the concept of ideal fluids with lines of vorticity having infinite core velocities would have to be replaced by a core structure determined from viscous flow considerations. Single vortex lines should also be replaced by a more realistic drop-off of circulation at the blade tip. Also, the blade itself can no longer be replaced by a lifting line, since the far wake in the vicinity of the leading edge has now very definitely become a near wake, and the more exact treatment reserved for the near wake must therefore be used for the entire wake. However, even without the introduction of such refinements, it is possible to draw some important qualitative conclusions from the results of the simpler analysis.

Following an analysis similar to the one just given, consider a rotor operating at an incidence angle of $-5°$. Under these conditions, using as a first trial the values for $\lambda_1/\lambda_0 = 0.5$ obtained previously, a new estimate for λ_1/λ_0 of $\lambda_1/\lambda_0 \simeq 0.9$ is obtained. A recomputation for the downwash using this value of λ_1/λ_0 results in a new value, at $\eta = 0.95$, of $\lambda_1/\lambda_0 = 1.28$. Evidently, as the leading edge of the spiral approaches the leading edge of the disk, the upwash is intensified and a mildy unstable condition exists in which the wake is drawn up into the leading edge of the rotor disk. This phenomenon is believed to be of considerable qualitative significance and, to a large part, accounts for the roughness in transition and flares experienced on most helicopters and the characteristic noise generated by rotors under conditions of wake interference. Many methods of alleviating this condition may be envisaged, for example, insuring as gradual a drop-off of circulation at the blade tips as possible without unduly sacrificing performance in order to reduce the intensity of the tip vortex. This may be done by moderating twist. Operationally, of course, the phenomenon may be greatly reduced by a climb-out or high acceleration through transition, a maneuver that will not always be possible. On tandem configurations, the possibility exists of using tow-out of the two tip path planes such that the front rotor provides most of the propulsive force, thereby operating at high inflows. The rear rotor, operating in the downwash of the front rotors, presents a lesser problem. As shown in Ref. 24, the transition vibration characteristics of a tandem configuration may be widely varied by adjustment of stagger and overlap.

Finally, the experimental results in Ref. 23 showed the marked reduction in the first harmonic inflow variations which occurs when the rotor is allowed to carry a moment at the hub. This is because the blade no longer equalizes lift around the azimuth and Γ_1 becomes appreciable, thereby producing a first harmonic downwash reducing the first harmonic upwash arising from γ_0. In practice, carrying large rolling or pitching moments produces high cyclic loads in the rotor system with attendant weight penalties. Furthermore, large offset of the flapping hinge with low blade Lock numbers is required, since the blade cannot be stiffened structurally sufficiently to prevent elimination of most of the cyclic lift change by elastic flapping. A discussion of this phenomenon is given in Ref. 25, together with estimates of the rolling moment as a function of the stall alleviation resulting from the cycle lift variations.

Determination of Rotor Loads

The computation of the rotor loads corresponding to the downwash variations just discussed is an involved process because of the necessity of satisfying the blade equilibrium equations. This becomes increasingly involved when the blade is close to resonance with one of the harmonics, a condition that is difficult to eliminate on present-day rotors. However, as discussed previously, experience with the solution of similar problems in the past and the results of the present computations indicate that the following simplified procedure may be used for computing blade loads.

First, trim requirements on single-rotor aircraft or structural requirements on multirotor aircraft dictate low first harmonic lift variations. This is achieved automatically by flapping on articulated rotors or by cyclic inputs on semirigid rotors. Consequently, γ_1 will always be small and its contribution to the harmonic content of the wake negligible, even though λ_{1c} is large. The lift alleviation by flapping decreases as the harmonic increases, as is evident from Eq. (18). However, the remaining wake harmonics are also small, always excepting the condition of wake suck-in at the leading edge. Consequently, their contribution to the harmonic content of the wake will also be small compared to that of the steady vortex lines due to γ_0. The wake structure is, therefore, dominated by the character of the steady-state circulation on the blade which produces the mean thrust, and the downwash produced by its vortex pattern will not be sensibly changed by the resulting harmonic lift changes on the blade. In computing higher harmonic air loads, it may, therefore, be assumed that the blade is subjected to an angle of attack established by the downwash due to γ_0, and, once this has been determined from consideration of its wake alone, no further iteration is necessary. In the case of harmonics above the second, it will be generally found that the blade motions may be neglected, always excepting the case of resonance, and the higher harmonic lift distribution computed from the angle-of-attack distribution given by the induced downwash of Eqs. (4).

The effect of the shed wake and time variations in the trailing wake strength may then be introduced, which will result in a further reduction of the effective lift curve slope in the presence of higher harmonic inputs, or an effective lift deficiency function.

Lift Deficiency Function in Forward Flight

It is of interest to examine the order of magnitude of $C(k)$, the lift deficiency, in forward flight for harmonic lift variations, and to compare the phase shift resulting from the spiral form of the wake with that occurring in the two-dimensional case. As a model, a harmonic variation in blade bound circulation will be assumed to be invariant with span, a condition somewhat approximating the test techniques employed in Ref. 16, in which the hub was displaced harmonically. All interharmonic coupling will be neglected.

For $\eta = 0.80$, $b/R = 0.05$, and $n = 3$, the reduced frequency is $nb/\eta R = 0.187$ and $I_c = 2.95$, $I_s = 1.29$, $I_c' = 2.05$, $I_s' = 1.21$.

Considering only the shed near wake, from Eq. (16), the circulation deficiency (which is somewhat less than the lift deficiency) is

$$\frac{\gamma_{3c}}{\gamma_{3c_q}} = \frac{1+S}{C^2 + (1+S)^2} = 0.675$$

and

$$\frac{\gamma_{3s}}{\gamma_{3c_q}} = \frac{C}{1+S}\,\frac{\gamma_{3c}}{\gamma_{3c_q}} = 0.298$$

where γ_{3c_q} is the "quasi-static" circulation and may be represented, for example, by the terms in brackets in Eq. (16).

The lift deficiency function for this case is then, from Eq. (17),

$$\frac{L_{3c}}{\rho V \Gamma_{3c_q}} = \left[-kI_c'\,\frac{\gamma_{3s}}{\gamma_{3c_q}} - kI_S'\,\frac{\gamma_{3c}}{\gamma_{3c_q}} + 1\right] = 0.734$$

$$\frac{L_{3s}}{\rho V \Gamma_{3c_q}} = \left[kI_c'\,\frac{\gamma_{3c}}{\gamma_{3c_q}} - kI_S'\,\frac{\gamma_{3c}}{\gamma_{3c_q}}\right] = 0.19$$

These values are readily verified as being the values for the conventional lift deficiency function of Ref. 25 for $k = 0.187$.

To this lift deficiency will now be added that due to the shed far wake. From numerical calculations of Eq. (11) and for $\mu = 0.10$, $A_{3c}{}^3 = 0.57$, $B_{3c}{}^3 = 3.39$, $A_{3s}{}^3 = -2.73$, and $B_{3s}{}^3 = 0.55$. The coefficient $nb/2R$ is 0.075 for the parameters just assumed, and Eq. (12) then gives, for the shed far wake only,

$$\lambda_{3c} = 0.043\,\gamma_{3s} + 0.205\,\gamma_{3c}$$

$$\lambda_{3s} = 0.254\,\gamma_{3s} - 0.041\,\gamma_{3c}$$

Since all interharmonic coupling has been neglected, a legitimate assumption when one harmonic predominates in the input, the circulation deficiency may now be computed directly from Eq. (16) with the preceding values of λ_{3c} and λ_{3s} substituted on the right-hand side.

The result is

$$\gamma_{3c}/\gamma_{3c_q} = 0.596 \qquad \gamma_{3s}/\gamma_{3c_q} = 0.234$$

The corresponding lift deficiency function is, from Eq. (17),

$$L_{3c}/\rho V \Gamma_{3c_q} = 0.734 - 0.043 \times 0.234 - 0.205 \times 0.596 = 0.602$$

$$L_{3s}/\rho V \Gamma_{3c_q} = 0.19 - 0.254 \times 0.234 + 0.041 \times 0.596 = 0.155$$

The effect of the trailing wake will now be considered. For the conditions chosen, $P_{3c}{}^3 = 6.07$, $Q_{3c}{}^3 = 2.51$, $P_{3s}{}^3 = 2.42$, and $Q_{3s}{}^3 = 6.78$.

Proceeding as before for the shed wake, Eq. (16) for the third harmonic components yields, for the complete wake,

$$\frac{\gamma_{3c}}{\gamma_{3c_q}} = 0.570 \qquad \frac{\gamma_{3s}}{\gamma_{3c_q}} = 0.186$$

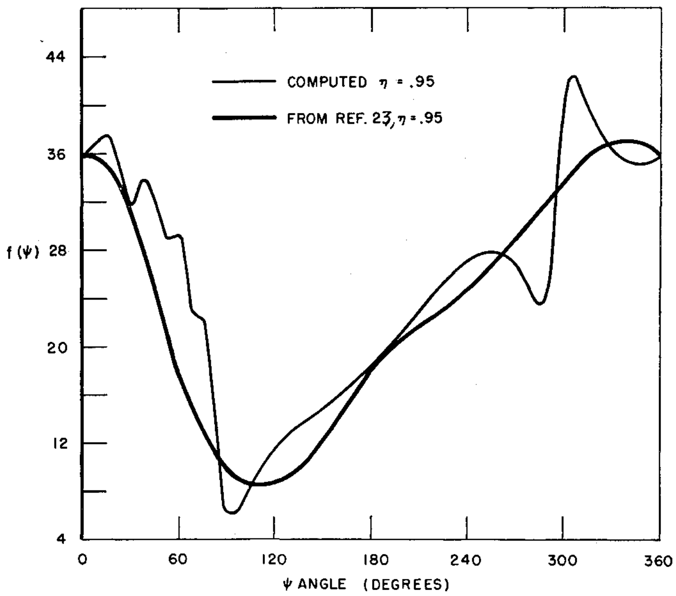

Fig. 8 Comparison of computed and experimental downwash (μ = 0.3, λ_1/λ_0 = 0.4).

The corresponding lift deficiency function is, from Eq. (17),

$$L_{3c}/\rho V\Gamma_{3c_q} = 0.602 + 0.06 \times 0.186 - 0.152 \times 0.570 = 0.525$$

$$L_{3s}/\rho V\Gamma_{3q} = 0.155 - 0.170 \times 0.186 - 0.06 \times 0.570 = 0.090$$

It is apparent from the foregoing that the near and far wakes contribute about equally to the lift deficiency, or reduction in slope of the lift curve, for the representative condition chosen.

It is of interest to compare the lift deficiency at μ = 0.1 just obtained with that predicted from the simplified hovering solution in closed form. The numerical computations at a given μ required definition of λ, Q, and b/R only. The corresponding value of h is

$$h = \frac{2\pi R\lambda}{Qb} = \frac{2\pi \times 0.05}{3 \times 0.025} = \frac{2\pi}{3}$$

and the lift deficiency function is, then, from Eq. (14),

$$1/[1 + (\pi/h)] = 0.40$$

Harmonic Content of the Downwash in Cruising Flight

In Fig. 7 are plotted the harmonic contents of the wake at μ of 0.3 due to the tip trailing vortex system for various harmonics. Of interest is the pronounced phase shift as evidenced by the relatively large sine components of downwash compared to the results at μ of 0.1.

Of particular interest is the persistence of the higher harmonic content at the higher advance ratio. At the lower advance ratio (Fig. 6), the higher harmonic induced flows are of the order of 20% of the steady-state induced flows. At the higher advance ratio (Fig. 7), the mean value over the blade span of the steady-state component of the induced flow has been appreciably reduced, as indicated by a comparison of $P_0{}^0$ from Figs. 6 and 7. This is as might be expected, since it is well known that, for a given lift, the induced flow decreases with forward speed. However, contrary to previous expectation, the higher harmonic components of induced flow have not been appreciably reduced, and, hence, the vibration level and also the blade fatigues stresses due to nonuniform downwash are not alleviated with increasing forward speed.

In Fig. 8, the downwash before harmonic analysis has been plotted against azimuth and compared with the experimentally determined downwash of Ref. 23. The two rotors are not strictly comparable; in particular, the rotor of Ref. 23 operated at appreciably lower inflows λ_0 than have been assumed here. However, at advance ratios of μ = 0.3, the effect of z, and hence λ_0, may be expected to be small compared to the effect of d, and hence μ, and the two results should be comparable, at least as regards distribution of inflow with respect to azimuth and span. Such a comparison can be made if both results are normalized at some azimuth position. ψ = 0, close to the point of a maximum downwash, has been selected for the common value. The agreement is excellent, and it may, therefore, be concluded that, as far as the lower harmonics are concerned, the mathematical model chosen for this analysis is adequate. The higher harmonics were attenuated in tests of Ref. 23, and consequently no direct comparison is possible between theory and experiment.

Conclusions

1) The nonuniform downwash induced at the rotor disk by the wake vortex system has a sufficient amount of higher harmonic content to account for the higher harmonic air loads encountered on rotor blades in forward flight. This higher harmonic content does not decrease with forward speed, as does the steady-state component of downwash.

2) The analysis and interpretation of the results are considerably simplified by dividing the wake into a "near" wake extending from the blade to approximately one-quarter of the disk aft and a "far" wake containing the rest of the spiral. The higher harmonic content of the downwash is due almost entirely to the far wake and particularly to that portion passing under the blade and generated either by itself or by another blade.

3) It follows from the previous conclusion that the harmonic air loads will be sensitive to the vertical spacing of the wake, and consequently it is necessary to introduce the concept of a nonrigid wake, particularly in low-speed transition flight or under any condition where the wake spacing is reduced such as in a flare. Under these conditions, the wake could be sucked up into the leading edge of the rotor disk, and it is believed that this is most probably the source of transition roughness and of the characteristic rotor noise encountered under certain flight regimes.

4) Unsteady aerodynamic effects are of considerable importance for the rotor because of the proximity of the returning wake to a blade. Analysis of these effects for the three-dimensional rotor is appreciably simplified if the far wake is treated using lifting-line theory, and lifting-surface theory is used only for the near wake. The validity of this approach has been demonstrated by comparing the equivalent treatment of a two-dimensional model of the returning wake system with a treatment using lifting-surface theory for both the far and near wakes.

5) In hovering flight, a simple closed-form solution is obtained for the reduction in lift due to unsteady aerodynamic effects by proceeding to the limiting case of an infinite number of blades. It is shown that, for normal rotor or rotor/propeller operating conditions, the harmonic lift generated by a cyclic change in blade pitch would be less than half that indicated by simple quasi-static theory, and that this reduction in lift is substantially independent of frequency.

Appendix: Two-Dimensional Solution for Oscillating Airfoil

The following very brief analysis is included in order to relate the treatment of the nonstationary flow effects contained in this paper to the classical analyses in the literature. Chapters 5 and 7 of Ref. 20 contain a complete development and review of both the two- and three-dimensional cases.

If the chordwise vorticity is represented by the series

$$\gamma(x) = A_0 \tan\frac{\theta}{2} + \sum_{n=1}^{\infty} A_n \sin n\theta \quad \text{(A1)}$$

and the distance from the center of the airfoil to a point aft on the airfoil is given by $x^* = b\cos\theta$, then the induced flow at x^* due to an element of vorticity on the airfoil at η is

$$dv(x) = \gamma(\eta)d\eta/2\pi(x^* - \eta) \quad \text{(A2)}$$

positive down, which, when integrated from $-b$ to $+b$, gives[29]

$$v(x) = \frac{A_0}{2} + \sum_{1}^{\infty} \frac{A_n}{2}\cos n\theta \quad \text{(A3)}$$

Assume now that the airfoil is moving with velocity V and has a velocity perpendicular to its surface $u(x)$ (positive down) at station x resulting from the angle of attack α (positive nose down) and the vertical velocity at the center of twist $\dot{z}$ (positive down). If the center of twist is located a distance ab aft from the center of the airfoil, then

$$u(x) = \alpha V - \dot{z} + (x^* - ab)\dot{\alpha}$$

Every change in circulation associated with these motions results in an element of vorticity $\gamma d\xi^*$ being shed at the trailing edge whose strength is equal and opposite to the change in bound circulation. Thus, $\gamma d\xi^* = -d\Gamma_b$, where ξ^* is the distance of the element of vorticity from the center of the airfoil, dimensional when starred. The velocity at the airfoil perpendicular to its surface induced by $\gamma d\xi^*$ is, for the sign convention of Fig. 3,

$$w(x) = -\gamma d\xi^*/2\pi(\xi^* - x^*) \quad \text{(A4)}$$

In the linearized solution the boundary conditions on the airfoil require that, for each element of vorticity in the wake,

$$v(x) + u(x) + w(x) = 0 \quad \text{(A5)}$$

or

$$\frac{A_0}{2} + \sum_{1}^{\infty}\frac{A_n}{2}\cos n\theta + [\alpha V - \dot{z} + (x^* - ab)\dot{\alpha}] - \frac{\gamma d\xi^*}{2\pi(\xi^* - x^*)} = 0 \quad \text{(A6)}$$

The Fourier coefficients A_n may be readily determined with the aid of Ref. 27, Table 63, formula 12, p. 99, from which is obtained

$$\int_0^{\pi} \frac{\cos n\theta}{\xi - \cos\theta}\,d\theta = \frac{\pi[\xi - (\xi^2 - 1)^{1/2}]^n}{(\xi^2 - 1)^{1/2}} \quad \text{(A7)}$$

whence

$$A_0 = \frac{\gamma d\xi}{\pi}\,\frac{1}{(\xi^2 - 1)^{1/2}} + 2(\dot{z} - \alpha V + ab\dot{\alpha})$$

$$\frac{A_1}{2} = \frac{\gamma d\xi}{\pi}\left[\frac{\xi}{(\xi^2 - 1)^{1/2}} - 1\right] - b\dot{\alpha} \quad \text{(A8)}$$

$$\frac{A_n}{2} = \frac{\gamma d\xi}{\pi}\,\frac{[\xi - (\xi^2 - 1)^{1/2}]}{(\xi^2 - 1)^{1/2}}$$

The incremental lift and moment on the airfoil due to the instantaneous displacements and in the presence of the flow field generated by $\gamma d\xi^*$ may now be computed for the vortex pair consisting of $\gamma d\xi^*$ and $d\Gamma_b$ on the airfoil, postulating that these are the only two elements of vorticity existing in the system. Bernoulli's equation extended to unsteady flow gives the pressure difference on the upper and lower surfaces as

$$(P_u - P_l) = -2\rho[(\partial\phi/\partial t)(x) + V(\partial\phi/\partial x^*)(x)] \quad \text{(A9)}$$

The second term includes the quasi-static effects arising from the instantaneous airfoil geometry, and the first term accounts for the time rate of change of velocity perpendicular to the airfoil, including apparent mass effects and those arising from the nonuniform velocity $w(x)$ at the airfoil due to $\gamma d\xi$ [Eq. (A2) and Fig. 3]. Therefore, when replacing the blade by a lifting line, terms in $\partial\phi/\partial t$ due to $\partial\xi/\partial t$ should be dropped. When $z \neq 0$, as in the far wake, $\partial\phi/\partial t$ will contain terms due to $\dot{z}$. However, in general, $\dot{z} \ll \dot{\xi}$, and its effects have therefore been neglected, except as they determine the instantaneous vertical position of $\gamma d\xi$ in the "semi-rigid" wake solutions.

The velocity potential, in terms of the distributed vorticity, is

$$\phi(x) = \tfrac{1}{2}\int_{-b}^{x^*} \gamma dx^*$$

whence

$$(\partial\phi/\partial x^*)(x) = \tfrac{1}{2}\gamma(x)$$

and

$$\frac{\partial\phi}{\partial t}(x) = \frac{1}{2}\frac{\partial}{\partial t}\int_{-b}^{x^*}\gamma(x)dx^*$$

The lift on the airfoil is

$$L = -\int_{-b}^{+b}(P_u - P_l)dx^*$$

and after substituting $\gamma(x)$ in the form given by Eq. (A1), the lift is obtained in terms of the coefficients A_n as

$$dL = \rho\pi b\{\tfrac{1}{2}(\partial/\partial t)(A_0 - \tfrac{1}{2}A_2)b + (\partial/\partial t)(A_0 + \tfrac{1}{2}A_1)b + V(A_0 + \tfrac{1}{2}A_1)\} \quad \text{(A10)}$$

The circulation on the airfoil is

$$d\Gamma = \int_{-b}^{+b}\gamma dx^* = \pi\left(A_0 + \frac{1}{2}A_1\right)b \quad \text{(A11)}$$

This is the lift and circulation on the airfoil at any instant due to the element of vorticity $\gamma d\xi$ in the wake and its counter vortex on the airfoil, $d\Gamma_b$. Since the rigid wake of constant strength is assumed, this element of vorticity in the wake has constant strength with time, or $(\partial/\partial t)(\gamma d\xi) = 0$. If the element of vorticity and the blade circulation $d\Gamma_b$ are to constitute a vortex pair, then

$$d\Gamma_b = -\gamma d\xi^*$$

and

$$(\partial/\partial t)d\Gamma = (\partial/\partial t)(A_0 + \tfrac{1}{2}A_1) = 0$$

which also defines the time history of airfoil motion required so that in moving a distance ξ^* after shedding the element of vorticity $\gamma d\xi^*$ no additional circulation has been generated by the airfoil. Then

$$dL = \rho\pi b\{\tfrac{1}{2}(\partial/\partial t)(A_0 - \tfrac{1}{2}A_2)b + V(A_0 + \tfrac{1}{2}A_1)\}$$

Differentiating the first term with respect to t and noting that $\partial/\partial t = (V/b)\,\partial/\partial\xi$ results in

$$dL = [\rho V\gamma d\xi/(\xi^2 - 1)^{1/2}] - 2\pi\rho Vb[\alpha V - \dot{z} + \dot{\alpha}(0.5b - a^*)] + \rho\pi(\ddot{z} - \dot{\alpha}V + a^*\ddot{\alpha})b^2$$

The first two terms represent the lift due to the vortex pair, of which the second term is the "quasi-static" lift L_q.

The third term represents the apparent mass and damping effects due to the noncirculatory flow. Integrating the first term for the effects of all elements of vorticity which have been shed from the start of the motion and leading to the present instantaneous airfoil position,

$$L = \rho V \int_1^\infty \frac{\gamma d\xi}{(\xi^2 - 1)^{1/2}} + L_q - \rho\pi(\dot{\alpha}V - \ddot{z} - a^*\ddot{\alpha})b^2 \tag{A12}$$

Similarly, the total circulation acting on the airfoil is, from (A11),

$$\Gamma_b = \int_1^\infty \left[\frac{\xi + 1}{(\xi^2 - 1)^{1/2}} - 1\right] \gamma d\xi - 2\pi b[\alpha V - \dot{z} - \dot{\alpha}(0.5b - a^*)]$$

and this must be equal and opposite to the total circulation in the wake, or

$$\Gamma_b = - \int_1^\infty \gamma d\xi$$

whence

$$\int_1^\infty \frac{\xi + 1}{(\xi^2 - 1)^{1/2}} \gamma d\xi = 2\pi b[\alpha V - \dot{z} - \dot{\alpha}(0.5b - a^*)] = - \frac{L_q}{\rho V} \tag{A13}$$

Combining Eqs. (A12) and (A13),

$$L = L_q \times \left[\int_1^\infty \frac{\xi\gamma d\xi}{(\xi^2 - 1)^{1/2}} \bigg/ \left(\int_1^\infty \frac{\xi\gamma d\xi}{(\xi^2 - 1)^{1/2}} + \int_1^\infty \frac{\gamma d\xi}{(\xi^2 - 1)^{1/2}}\right)\right] - \rho\pi b^2(\dot{\alpha}V - \ddot{z} - a^*\ddot{\alpha})$$

If the displacements z and α vary harmonically with time, then L will also be of the form $L = L_0 e^{i\omega t}$, and, as was done in the body of this paper, the first term may be readily identified as the classical lift deficiency function $C(k)$.

The incremental moment about the center of twist acting on the airfoil is

$$dM = \int_{-b}^{+b} (P_u - P_l)(x^* - ba)dx^* = abdL - \frac{\pi\rho}{4} b^2 \left\{b \frac{\partial A_0}{\partial t} + \frac{3}{4} b \frac{\partial A_1}{\partial t} - \frac{1}{4} b \frac{\partial A_3}{\partial t} - V(2A_0 - A_2)\right\}$$

After substituting for the coefficients A_n and their time derivatives,

$$dM = abdL + \frac{\rho V b^2 \gamma d\xi}{2(\xi^2 - 1)^{1/2}} + \frac{\pi\rho\ddot{\alpha}b^4}{8} - \rho\pi V(\alpha V - \dot{z} - ab\dot{\alpha})b^2$$

Adding dL from the previous analysis and summing up over the entire wake gives

$$M = -\rho V b^2 \int_1^\infty \frac{\xi a - 0.5}{(\xi^2 - 1)^{1/2}} \gamma d\xi - \rho\pi[\dot{\alpha}V - \ddot{z} - ab\ddot{\alpha}]ab^3 + \rho \frac{\pi\ddot{\alpha}b^4}{8} - \rho\pi V(\alpha V - \dot{z} - ab\dot{\alpha})b^2$$

Substituting Eq. (A13) results in

$$M = L_q(a + 0.5) \times \left[\int_1^\infty \frac{\xi\gamma d\xi}{(\xi^2 - 1)^{1/2}} \bigg/ \int_1^\infty \frac{\xi\gamma d\xi}{(\xi^2 - 1)^{1/2}} + \int_1^\infty \frac{\gamma d\xi}{(\xi^2 - 1)^{1/2}}\right] + \rho\pi a(\ddot{z} + ab\ddot{\alpha})b^3 + \rho\pi V\dot{\alpha}(0.5 - a)b^3 + \frac{\rho\pi\ddot{\alpha}b^4}{8} \tag{A14}$$

Examination of Eq. (A14) and the expression for L_q,

$$L_q = -2\pi\rho V b[\alpha V - \dot{z} + \dot{\alpha}b(0.5 - a)]$$

indicates that the forces and moments acting on the oscillating airfoil may be resolved into the following components: 1) a force acting at the 25% chord due to the angle of attack at the 75% chord (rear neutral point) and multiplied by $C(k)$; 2) a force due to the angular velocity $\dot{\alpha}$ of the airfoil acting at the 75% chord point and given by $\rho\pi V\dot{\alpha}b^2$; and 3) a force due to the apparent mass term, $\pi\rho b^2\ddot{z}$, acting at the center of the airfoil, and a moment $\pi\rho b^4\ddot{\alpha}/8$. Identification of the forces and moments in this manner frequently permits a considerable amount of simplification in handling the aerodynamic coupling terms when $\dot{\alpha}b(0.5 - a) \ll \dot{z}$, as is generally the case for helicopter rotor blades. This point is discussed further in Ref. 3.

References

[1] Loewy, R. G., "A two dimensional approach to the unsteady aerodynamics of rotary wings," J. Aerospace Sci. **24**, 82–98 (1957).

[2] Daughaday, H. and Kline, J., "An approach to the determination of higher harmonic rotor blade stresses," Proceedings of the 9th Annual Forum, American Helicopter Society (1953).

[3] Miller, R. H. and Ellis, C. W., "Blade vibration and flutter," J. Am. Helicopter Soc. **1**, 19–38 (July 1956).

[4] Coleman, R. P., Feingold, A. M., and Stempin, C. W., "Evaluation of the induced velocity field of an idealized helicopter rotor," NACA ARR L5E10 (WRL 126) (June 1945).

[5] Mangler, K. W., "Calculation of the induced velocity field of a rotor," Royal Aircraft Establishment Rept. 2247 (February 1948).

[6] Castles, W. and deLeeuw, J. H., "The normal component of the induced velocity in the vicinity of a lifting rotor and some lexample of its application," NACA TR1184 (1954).

[7] Heyson, H. H. and Katzoff, S., "Induced velocities near a ifting rotor with non-uniform disk loading," NACA TR 1319 (1957).

[8] Heyson, H. H., "Tables and charts of the normal component of induced velocity in the lateral plane of a rotor with harmonic azimuthwise vorticity distribution," NASA TN D-809 (April 1961).

[9] Dress, J. M., "A theory of airflow through rotors and its application to some helicopter problems," J. Helicopter Assoc. Gt. Brit. **3**, 79–104 (July–September 1949).

[10] Willmer, M. A. P., "The loading of helicopter rotor blades in forward flight," Royal Aircraft Establishment Rept. Naval 2-N-76935, no. 8 (April 1959).

[11] Castles, W. and Durham, W. L., "The computed instantaneous velocities induced at the blade axes by the skewed helical vortices in the wake of a lifting rotor in forward flight," Armed Services Technical Information Agency Doc. AD-21013 (March 1959).

[12] Jones, J., "The influence of the wake on the flutter and vibration of rotor blades," British Aeronautical Research Council Rept. 18, 173 (January 1956).

[13] Timman, R. and van de Vorren, A. I., "Flutter of a helicopter rotor rotating in its own wake," J. Aerospace Sci. **24**, 694–702 (1957).

[14] Ashley, H., Moser, H. H., and Dugundji, J., "Three dimensional effects on unsteady flow through a helicopter rotor," Wright Air Development Center Rept. 58-87, Part III (October 1958).

[15] Miller, R. H., "Aeroelastic effects on helicopter and VTOL aircraft rotor design," Chap. II of notes on Special Summer Program in Aeroelasticity, Massachusetts Institute of Technology (1958).

[16] Zvara, J., Ham, N. D., and Moser, H. H., "Investigation of rotor response to vibratory aerodynamic inputs—experimental results and correlation with theory," Wright Air Development Center Rept. 58-87, Part I (October 1958).

[17] Theodorsen, T., "General theory of aerodynamic instability and the mechanism of flutter," NACA TR 496 (1935).

[18] von Kármán, T. and Sears, W. R., "Airfoil theory for nonuniform motion," J. Aeronaut. Sci. **5**, 379–390 (1938).

[19] Kussner, H. G., "Comprehensive report on the non-stationary

lift of airfoils," Luftfahrtforschung **13**, 411–423 (December 20, 1936).

[20] Bisplinghoff, R. L., Ashley, H., and Halfman, R., *Aeroelasticity* (Addison-Wesley Publishing Co., Inc., Reading, Mass., 1955).

[21] Glauert, H., "The force and moment on an oscillating airfoil," Aeronautical Research Council R and M 1242 (1929).

[22] Brotherhood, P. and Stewart, W., "An experimental investigation of the flow through a helicopter rotor in forward flight," Aeronautical Research Council R and M 2734 (September 1949).

[23] Falabella, G. and Meyer, J. R., "Determination of inflow distributions from experimental aerodynamic loading and blade motion data on a model helicopter rotor in hovering and forward flight," NACA TN 3492 (November 1955).

[24] Duvivier, J. F., "Study of helicopter rotor-rotor interference effects on hub vibrations," Massachusetts Institute of Technology ASRL TR 95-1 (October 1961).

[25] Miller, R. H., "Some factors affecting the design and future operation of helicopters," Proceedings of the 4th Anglo-American Aeronautical Conference, London (1953).

[26] Pierce, F., *A Short Table of Integrals* (Ginn and Co., Boston, Mass., 1956).

[27] Bierens, de Haan, D., *Nouvelles Tables d'Integrales Definies* (Stechert and Co., New York, 1939).

[28] Gessow, A. and Myers, G. C., Jr., *Aerodynamics of the Helicopter* (Macmillan Co., New York, 1952).

[29] Glauert, H., *Airfoil and Airscrew Theory* (Cambridge University Press, Cambridge, England, 1930), Chap. VII.